10436
NACA TN 4102
TECH LIBRARY KAFB, NM
0066972

NATIONAL ADVISORY COMMITTEE FOR AERONAUTICS

TECHNICAL NOTE 4102

VELOCITY AND FRICTION CHARACTERISTICS OF LAMINAR VISCOUS BOUNDARY-LAYER AND CHANNEL FLOW OVER SURFACES WITH EJECTION OR SUCTION

By E. R. G. Eckert, Patrick L. Donoughe, and Betty Jo Moore

Lewis Flight Propulsion Laboratory
Cleveland, Ohio

Washington
December 1957

TECHNICAL LIBRARY
AFL 2811

TECH LIBRARY KAFB, NM

0066972

NATIONAL ADVISORY COMMITTEE FOR AERONAUTICS

TECHNICAL NOTE 4102

VELOCITY AND FRICTION CHARACTERISTICS OF LAMINAR VISCOUS BOUNDARY-LAYER AND CHANNEL FLOW OVER SURFACES WITH EJECTION OR SUCTION

By E. R. G. Eckert, Patrick L. Donoughe, and Betty Jo Moore

4518

CY-1

SUMMARY

Information collected from the referenced literature and supplemented by new solutions is presented on the flow characteristics - velocity field, pressure drop, and friction - for steady, fully developed laminar flow through a duct consisting of two parallel walls, for flow through tubes with circular cross section, and for boundary-layer flow over infinite wedges. It is assumed that the fluid either is ejected through the porous walls into the main flow or is removed from the main flow by suction. The properties of the fluid both in the main flow and in passing through the porous walls are assumed constant, identical, and incompressible.

In order to determine the extent to which the boundary conditions imposed on the flow by the various geometries influence the flow characteristics, dimensionless parameters common to both channel and boundary-layer flow (channel flow is flow with bounding walls, e.g., a tube) were developed. By using these parameters to compare the various flows, the flow on surfaces with fluid ejection as well as on solid surfaces was found to depend mainly on the local boundary-layer thickness, on the pressure gradient in main-flow direction, and on the ejection rates. Whether the viscous flow is confined in a channel or unconfined in a boundary layer is of secondary importance. This finding forms the basis for general correlations and shows the conditions under which data on channel and boundary-layer flow are interchangeable; it also should be useful for calculations by integral methods.

INTRODUCTION

In the search for effective cooling methods, attention has been directed towards a method known as transpiration cooling. In this method, the surfaces to be protected against the influence of a hot fluid stream are manufactured from a porous material, and a cold fluid is ejected through the wall to form a protective layer along the surface. Certain

areas on the skin of high-velocity aircraft may be provided with these surfaces as protection against the influence of aerodynamic heating. Porous surfaces with suction also are used on airfoils and bodies of aircraft to delay separation or transition to turbulence; in these cases, the flow along the surface is of a boundary-layer type. In nuclear applications, the protection of the channel walls by transpiration cooling is of primary interest.

As a result of these applications, numerous studies of the flow and heat transfer connected with fluid ejection or suction through porous surfaces have been made recently. Analytical investigations cover laminar two-dimensional steady boundary-layer flow (ref. 1), laminar flow through ducts bounded by two parallel walls with one or both walls porous (refs. 2 to 4), and laminar flow through tubes with circular cross section (ref. 5). Semiempirical treatments deal also with turbulent boundary-layer flow over porous surfaces (refs. 6 to 11).

The laminar-flow characteristics determined in these studies differ markedly from one geometry to the other. For instance, the velocity profiles in laminar boundary-layer flow over a flat plate become S-shaped as soon as fluid is ejected through the wall into the main stream, and the wall shear stress and the friction factor decrease with increasing ejection rate. In laminar flow through a circular tube, on the other hand, the velocity profiles become fuller, and the wall shear stress and the friction factor increase with increasing ejection rate. An investigation of the reasons for these differences in flow behavior and of the order of importance of the parameters influencing the velocity fields (and the friction characteristics) in the various geometries would provide a better understanding of the interplay of forces surrounding the flow-process development. It also would provide specific geometry generalizations applicable to other configurations.

This report presents the results of such a study conducted at the NACA Lewis laboratory for laminar boundary-layer and channel flow. The parameters used were dimensionless pressure gradient, friction factor, and flow rate through the porous walls. In order to compare the different flow geometries, solutions were obtained for flow with fluid ejection or suction through the walls of a circular tube and through one or both walls of a duct bounded by two parallel walls. These solutions were obtained on an IBM 650 electronic computer and are given in this report; a few numerical cases for laminar boundary-layer flow with fluid ejection also are included. The flow characteristics described by these solutions and by solutions available in the literature were analyzed in the manner described in the preceeding paragraph.

4518

CY-1 back

SOLUTION OF THE DIFFERENTIAL EQUATIONS

Laminar-Flow Equations

In all of the flow configurations, the following conditions are assumed: that the fluid is incompressible, that the properties of the fluid and of the coolant are constant, that the main-stream fluid and the fluid passing through the wall have identical properties. Two-dimensional flow is preserved in the viscous boundary layer and in the duct. With two-dimensional flow, the width is much greater than the height in the duct. In the present report, the term channel flow signifies flow in rectangular ducts as well as in circular tubes. The term duct flow is restricted to flow in a passage of rectangular cross section. Fully developed flow is assumed in the channels; the meaning of this term for channels with fluid ejection will be discussed later in the report. Rotational symmetry is assumed for flow through a tube, and steady state is postulated in all cases. In boundary-layer flow, a wedge-type flow (flow with a velocity outside the boundary layer proportional to some power of the distance from the leading edge) is considered. Such a main-stream velocity distribution is established in flow over a wedge of infinite extent.

Throughout this section, the equations are numbered to indicate by suffix the type of geometry used: no suffix will indicate the fully porous channel; suffix a, the semiporous channel; suffix b, the tube; and suffix c, the wedge. (Thus, eq. (1b) shows tube geometry, (1c) wedge flow, etc.)

Rectangular duct. - For the duct geometry (fig. 1(a) and (b)), the foregoing assumptions allow the Navier-Stokes equations of motion to be written as (e.g., ref. 12, p. 48)

$$u \frac{\partial u}{\partial x} + v \frac{\partial u}{\partial y} = - \frac{1}{\rho} \frac{\partial p}{\partial x} + \nu \left(\frac{\partial^2 u}{\partial x^2} + \frac{\partial^2 u}{\partial y^2} \right) \tag{1}$$

$$u \frac{\partial v}{\partial x} + v \frac{\partial v}{\partial y} = - \frac{1}{\rho} \frac{\partial p}{\partial y} + \nu \left(\frac{\partial^2 v}{\partial x^2} + \frac{\partial^2 v}{\partial y^2} \right) \tag{2}$$

The continuity equation is

$$\frac{\partial u}{\partial x} + \frac{\partial v}{\partial y} = 0 \tag{3}$$

Symbols are defined in appendix A.

Tube. - For flow through a tube (fig. 1(c)), the equations of motion are stated in cylindrical coordinates (e.g., ref. 12, p. 49):

$$u \frac{\partial u}{\partial x} + v \frac{\partial u}{\partial r} = - \frac{1}{\rho} \frac{\partial p}{\partial x} + \nu \left(\frac{\partial^2 u}{\partial r^2} + \frac{1}{r} \frac{\partial u}{\partial r} + \frac{\partial^2 u}{\partial x^2} \right) \tag{1b}$$

$$u \frac{\partial v}{\partial x} + v \frac{\partial v}{\partial r} = - \frac{1}{\rho} \frac{\partial p}{\partial r} + \nu \left(\frac{\partial^2 v}{\partial x^2} + \frac{\partial^2 v}{\partial r^2} + \frac{1}{r} \frac{\partial v}{\partial r} - \frac{v}{r^2} \right) \tag{2b}$$

4518

The continuity equation is

$$\frac{\partial (ru)}{\partial x} + \frac{\partial (rv)}{\partial r} = 0 \tag{3b}$$

Boundary-layer flow. - For the boundary-layer flow over wedges, (fig. 1(d)) the simplifications to the Navier-Stokes equations proposed by Prandtl are used. The equations then become (ref. 12, chap. VII)

$$u \frac{\partial u}{\partial x} + v \frac{\partial u}{\partial y} = - \frac{1}{\rho} \frac{\partial p}{\partial x} + \nu \frac{\partial^2 u}{\partial y^2} \tag{1c}$$

$$\frac{\partial p}{\partial y} \approx 0 \tag{2c}$$

$$\frac{\partial u}{\partial x} + \frac{\partial v}{\partial y} = 0 \tag{3c}$$

Boundary conditions. - For the boundary conditions, the main-flow velocity u is specified as zero at the solid or porous boundary, and the velocity normal to the wall may be either zero or a constant negative or positive value.

For the fully porous rectangular duct, the flow is symmetrical about the midchannel, so that only half the channel need be considered. The boundary conditions are

$$\left.\begin{aligned} y_2 &= 0 (\text{midchannel});\ v = 0;\ \frac{\partial u}{\partial y_2} = 0 \\ y_2 &= \frac{h}{2}\ (\text{porous wall});\ v = v_w;\ u = 0 \end{aligned}\right\} \tag{4}$$

4518

For the semiporous channel,

$$\left.\begin{aligned} y_1 &= 0 \text{ (solid wall)}; \; v = 0; \; u = 0 \\ y_1 &= h \text{ (porous wall)}; \; v = v_w; \; u = 0 \end{aligned}\right\} \tag{4a}$$

In the porous tube,

$$\left.\begin{aligned} r &= 0 \text{ (midtube)}; \; v = 0; \; \frac{\partial u}{\partial r} = 0 \\ r &= R \text{ (porous wall)}; \; v = v_w; \; u = 0 \end{aligned}\right\} \tag{4b}$$

For the viscous flow over a wedge,

$$\left.\begin{aligned} y_b &= 0 \text{ (porous wall)}; \; v = v_w; \; u = 0 \\ y_b &\rightarrow \infty \text{ (main stream)}; \; u \rightarrow u_m \end{aligned}\right\} \tag{4c}$$

Similarity Transformations

The references show that solutions for a special set of boundary conditions can be found for all differential equations presented in the preceding section. These solutions are characterized by similar velocity profiles at various x-locations. For channel flow this similarity is consistent with a constant ejection or suction velocity v_w. For such flow, this condition either restricts the shape of the velocity profile in a selected upstream cross section or assumes a selected upstream distance that is analogous to the fully established flow condition in a duct with solid walls. In channels with fluid ejection, the similarity in velocity profiles is encountered when the channel is closed at some upstream cross-section location that can be calculated. In boundary-layer wedge flow, the same condition requires that v_w vary in a specified manner in x-direction.

The partial differential equations describing the flow can be transformed under the specified conditions into total differential equations by the introduction of proper new variables. The continuity equation is automatically satisfied by a stream function ψ, which is different for each of the geometries. The equations of motion then can be transformed to ordinary differential equations by the use of a dimensionless length coordinate and a dimensionless stream function f that is postulated to

be a function only of the dimensionless normal distance η. Both parameters are connected with the previously used variables according to the following transformations:

Fully porous duct	Semiporous duct	Tube	Boundary layer
$\eta_2 = \frac{2y_2}{h}$	$\eta_1 = \frac{y_1}{h}$	$\eta_t = \left(\frac{r}{R}\right)^2$	$\eta_b = \frac{y_b}{x}\sqrt{Re_b}$
$\psi_2 = \frac{h}{2}\bar{u}(x)f_2(\eta_2)$	$\psi_1 = h\bar{u}(x)f_1(\eta_1)$	$\psi_t = R^2\bar{u}(x)f_t(\eta_t)$	$\psi_b = \sqrt{\nu x u_m}\, f_b(\eta_b)$

4518

Total Differential Equations

Substitution of the new variables η and f in the appropriate equations of motion resulted in the following total differential equations. The boundary conditions, given by equation (4), are also presented in terms of the new variables. The references mentioned with each geometry present the derivation of the equations in detail.

Fully porous duct (refs. 2 and 3):

$$f_2''' + \frac{Re_{d,w}}{2}\left(f_2'^2 - f_2 f_2''\right) = A_2 \tag{5}$$

where

$$Re_{d,w} \equiv \frac{v_w h}{\nu}$$

$$\left.\begin{aligned} \eta_2 &= 0 \text{ (midchannel)};\ f_2 = 0;\ f_2'' = 0 \\ \eta_2 &= 1 \text{ (porous wall)};\ f_2 = 1;\ f_2' = 0 \end{aligned}\right\} \tag{6}$$

Semiporous duct (refs. 3 and 4):

$$f_1''' + Re_{d,w}\left(f_1'^2 - f_1 f_1''\right) = A_1 \tag{5a}$$

$$\left.\begin{aligned} \eta_1 &= 0 \text{ (solid wall)};\ f_1 = 0;\ f_1' = 0 \\ \eta_1 &= 1 \text{ (porous wall)};\ f_1 = 1;\ f_1' = 0 \end{aligned}\right\} \tag{6a}$$

Tube (ref. 5):

$$\eta_t f_t''' + f_t'' + Re_{t,w}(f_t'^2 - f_t f_t'') = A_t \tag{5b}$$

where

$$Re_{t,w} \equiv \frac{v_w R}{\nu}$$

$$\left.\begin{aligned} &\eta_t = 0 \text{ (midtube)};\ f_t = 0;\ \eta_t f_t''' = 0 \\ &\eta_t = 1 \text{ (porous wall)};\ f_t = 1/2;\ f_t' = 0 \end{aligned}\right\} \tag{6b}$$

It should be noted that the solution of equation (5b) as given in reference 5 does not use the boundary condition $\eta_t f_t'''(0) = 0$. Instead, $\lim_{\eta_t \to 0} \sqrt{\eta_t}\, f_t'' = 0$, which stems from equations (4) to (6) herein and is fulfilled by the perturbation solution of reference 5, is used. Such a condition apparently allows $f_t''(0)$ to take on any value in a numerical solution and, hence, is not useful in the numerical solution. It has been replaced by the stated boundary condition, which satisfies the differential equation for $f_t'''(0)$ finite. Then the condition $\lim_{\eta_t \to 0} \sqrt{\eta_t}\, f_t'' = 0$ for $f''(0)$ finite is also satisfied.

The symbol A in equations (5) is an integration constant and, as will be shown later, is related to the pressure drop in x-direction.

Wedge (ref. 13):

$$f_b''' + \frac{Eu + 1}{2} f_b f_b'' - Eu(f_b'^2 - 1) = 0 \tag{5c}$$

$$\left.\begin{aligned} &\eta_b = 0 \text{ (porous wall)};\ f_b = f_{b,w};\ f_b' = 0 \\ &\eta_b \to \infty;\ f_b' \to 1 \end{aligned}\right\} \tag{6c}$$

In the channel-flow equations, the wall Reynolds number Re_w is a measure of the ejection rate for the channel and the tube.

In the boundary-layer or wedge flow, the dimensionless parameter called the Euler number

$$Eu = \frac{-x \frac{\partial p}{\partial x}}{\rho u_m^2} \tag{7}$$

is a measure of the pressure gradient, and the dimensionless grouping

$$f_{b,w} = \frac{-2}{Eu + 1} \frac{v_w}{u_m} \sqrt{Re_{b,x}} \tag{8}$$

characterizes the ejection rate. Equation (8) also prescribes the variation of the velocity v_w with the distance in main-flow direction x, since $f_{b,w}$ is independent of x:

$$v_{b,w} \propto x^{\frac{Eu - 1}{2}}$$

Method of Solution and Results

Perturbation solutions of equations (5), (5a), and (5b) are given in references 2, 4, and 5, respectively. These solutions are valid only for either large or small values of Re_w. For a study of the flow at intermediate values of Re_w, a numerical integration method was employed for the solution of these equations.

Equations (5), (5a), and (5b), together with the associated boundary conditions, constitute a nonlinear boundary-value problem with the parameter Re_w. Each of these equations was solved by an iterative method using the IBM 650 computer. The machine input values for the three equations were estimates for the following parameters: A_2 and $f_2'(0)$ in equation (5), A_1 and $f_1''(0)$ in equation (5a), A_t and $f_t''(1)$ in equation (5b). In the solution for the tube, the equation was integrated from $\eta = 1$ to $\eta = 0$ because the integrating technique required finding the value of the high-order derivative for the first five points, and because difficulty was encountered in evaluating $f_t'''(0)$.

Each iteration consisted of an integration using five-point formulas and a subsequent machine calculation for the next trial values. The iteration process was stopped as soon as the boundary conditions were

correct to four decimal places. This same technique was used for all three equations. The five-point integration is described in detail by Albers in appendix B of reference 14.

A comparison of the present results with those found in the literature is given in appendix B of the present report. The modifications required to overcome specific obstacles in the solution of equations (5), (5b), and (5c) are discussed in appendix C. An analogy between boundary-layer flow near the separation point and channel flow near a wall shear stress of zero also is suggested in appendix C.

4518

The results of the numerical solutions are presented in tables I to IV, with the values of f and its derivatives tabulated as functions of η. In addition to the tables, a representative solution for each geometry is given in figure 2. This figure illustrates the behavior of the functions when the geometry is changed. No common ground appears to exist in the changes from one geometry to another.

Relations Between Tabulated Functions and Physical Quantities

C1-2

The functions f (e.g., f_1, f_2, f_b', etc.) can be interpreted in terms of quantities with evident physical meaning.

Velocity. - The tabulated function f is connected with the stream function ψ. Therefore, the first derivative f' can be related to the velocity as follows:

By using the appropriate transformation and equation (3),

$$f_2' = \frac{u}{\bar{u}(x)}; \quad f_{2,m}' = \frac{u_m}{\bar{u}(x)} \tag{9}$$

$$f_1' = \frac{u}{\bar{u}(x)}; \quad f_{1,m}' = \frac{u_m}{\bar{u}(x)} \tag{9a}$$

$$2f_t' = \frac{u}{\bar{u}(x)}; \quad 2f_{t,m}' = \frac{u_m}{\bar{u}(x)} \tag{9b}$$

$$f_b' = \frac{u}{u_m} \tag{9c}$$

where, in channel flow,

$$[\bar{u}(x)]_2 = \bar{u}(0)\left(1 - \frac{4Re_{d,w}x}{Re_{2,0}h}\right) \tag{10}$$

$$[\bar{u}(x)]_1 = \bar{u}(0)\left(1 - \frac{2Re_{d,w}x}{Re_{1,0}h}\right) \tag{10a}$$

4518

$$[\bar{u}(x)]_t = \bar{u}(0)\left[\frac{1}{f_t'(0)} + \frac{4Re_{t,w}x}{Re_{t,0}R}\right] \tag{10b}$$

and $\bar{u}(0)$ is the average velocity at an arbitrarily assigned location $x = 0$. Equations (9) and (10) illustrate one of the fundamental differences between the bounded channel flow and the free boundary-layer flow. For bounded flow, the maximum velocity u_m is dependent upon the amount of suction or blowing, whereas such an interdependence does not exist for the boundary layer between the free-stream velocity u_m and the ejection or suction rate.

Pressure gradient. - The results given in references 2 to 5 show that the integration constant A is a measure of the pressure gradient in the main-flow direction. For example, using equation (9) in reference 4 gives the following equation for the semiporous channel:

$$\frac{\partial p}{\partial x} = \rho\bar{u}(x)\left[\frac{v_w}{h}\left(f_1'^2 - f_1 f_1''\right) + \frac{\nu}{h^2} f_1'''\right]$$

Thus, using equation (5a) herein and substituting (see SYMBOLS),

$$\frac{Re_1 h}{\rho\bar{u}^2(x)}\frac{\partial p}{\partial x} = 2A_1 \tag{11a}$$

In a similar manner, the equation for the fully porous channel

$$\frac{Re_2 h}{\rho\bar{u}^2(x)}\frac{\partial p}{\partial x} = 8A_2 \tag{11}$$

and, for the porous tube,

$$\frac{Re_t R}{\rho\bar{u}^2(x)}\frac{\partial p}{\partial x} = 16A_t \tag{11b}$$

may be obtained.

Shear stress. - The shear stress of a flowing fluid at a bounding wall is given by

$$\tau_w = \mu \left(\frac{\partial u}{\partial y}\right)_w = \mu \left(\frac{\partial u}{\partial \eta}\right)_w \left(\frac{\partial \eta}{\partial y}\right) \tag{12}$$

Use of equations (9) and the definition of η in conjunction with equation (12) results in

$$\tau_{2,w} = \frac{2\mu\bar{u}(x)}{h} f''_{2,w} \tag{13}$$

$$\tau_{1,w} = \frac{\mu\bar{u}(x)}{h} f''_{1,w} \tag{13a}$$

$$\tau_{t,w} = \frac{4\mu\bar{u}(x)}{R} f''_{t,w} \tag{13b}$$

$$\tau_{b,w} = \frac{\mu u_m \sqrt{Re_x}}{x} f''_{b,w} \tag{13c}$$

for the various geometries.

COMMON PARAMETERS FOR BOUNDARY-LAYER AND CHANNEL FLOW

From information available for boundary-layer flow along a surface with fluid ejection, the local flow conditions, as described by the shape of the velocity profile and by the local shear stress, are known to be functions mainly of the local pressure gradient, the local blowing rate, and the local boundary-layer thickness. The previous history of the boundary layer is of minor importance unless sudden stepwise variations in one of the parameters occur just upstream of the location under consideration. The boundary-layer thickness can be eliminated as a parameter by expressing the pressure gradient and the blowing rate in dimensionless form with the boundary-layer thickness used as a characteristic length.

It may be suspected from this knowledge that the differences between channel flow and boundary-layer flow will be minimized where the comparison is made on the basis of these parameters; this comparison is carried out in the next section. In this section, the following common dimensionless parameters for boundary layer and for duct flow are developed and expressed in terms of the parameters previously used:

4518
CY-2 back

Dimensionless boundary-layer thickness:

$$Re_{\delta^*} \equiv \frac{u_m \delta^*}{\nu} \tag{14}$$

Dimensionless ejection rate:

$$\Phi \equiv \frac{v_w}{u_m} Re_{\delta^*} \tag{15}$$

4518

Dimensionless pressure gradient:

$$\Pi_x \equiv \frac{Re_{\delta^*}\delta^*}{\rho u_m^2} \frac{\partial p}{\partial x} \tag{16}$$

Dimensionless friction factor:

$$T \equiv \frac{\tau_w}{\frac{1}{2} \rho u_m^2} Re_{\delta^*} \tag{17}$$

The displacement Reynolds number Re_{δ^*} appears in each grouping and, as will be seen later, allows the evaluation of Φ, Π_x, and T from numerical solutions of the differential equations.

Boundary-Layer Flow

The dimensionless parameters expressing the ejection or suction $f_{b,w}$, the pressure gradient Eu, and the shear stress at the wall $C_w \frac{\sqrt{Re_x}}{2}$ are based on the length x (ref. 13) and can be converted to parameters that utilize the boundary-layer displacement as defined by

$$\delta^* = \int_0^\infty \left(1 - \frac{u}{u_m}\right) dy = \frac{x}{\sqrt{Re_x}} \int_0^\infty (1 - f_b') \, d\eta_b \tag{18}$$

Denoting the parameter $\frac{\delta^* \sqrt{Re_x}}{x}$ by B,

$$Re_{\delta^*} = B\sqrt{Re_x} \tag{19}$$

where $B \equiv \int_0^\infty (1 - f_b') \, d\eta_b$.

The ejection parameter Φ_b (eq. (15)), which uses the boundary-layer displacement thickness δ^* (as Re_{δ^*}), becomes

$$\Phi_b = \frac{-v_{b,w}}{u_m} B\sqrt{Re_x} = B\,\frac{Eu + 1}{2}\,f_{b,w} \tag{20}$$

The velocity $v_{b,w}$ is positive for fluid ejection with boundary-layer flow and negative for the channels, according to the notation introduced before. The minus sign is inserted in equation (20) in order to make Φ_b positive for suction in all configurations. The value of Φ_b can be calculated from the results in table V and is given therein.

4518

To obtain a dimensionless parameter for the pressure drop $\partial p/\partial x$, δ^* is substituted for x in the Euler number. From equation (19),

$$x = \delta^* Re_{\delta^*}/B^2$$

and, from equation (7),

$$Eu = \frac{-\delta^* Re_{\delta^*} \frac{\partial p}{\partial x}}{B^2 \rho u_m^2} \tag{21}$$

The pressure-drop parameter $\Pi_{x,b}$ (eq. (16)) is

$$\Pi_{b,x} = -B^2\,Eu \tag{22}$$

a parameter that can be calculated from table V and is given therein.

The shear stress is given by equation (13c). Replacing x by δ^* results in

$$f''_{b,w} = \frac{\tau_{b,w}}{\rho u_m^2}\,\frac{Re_{\delta^*}}{B} \tag{23}$$

The dimensionless friction parameter (eq. (17)) is

$$T_b = 2Bf''_{b,w} \tag{24}$$

and may be calculated from table IV; results are given in table V.

Channel Flow

In order to obtain channel-flow parameters that are analogous to those for boundary-layer flow, a velocity analogous to u_m and a length analogous to δ^* must be chosen. It is reasonable to use the maximum velocity u_m in the channel cross section under consideration as the characteristic velocity. An equivalent boundary-layer thickness δ^* for channel flow can be obtained from the equation

$$\delta^* = \int_0^{y_m} \left(1 - \frac{u}{u_m}\right) dy \tag{25}$$

where the integral is extended from the wall under consideration to the distance y_m where the maximum velocity occurs.

Fully porous duct. - For the fully porous duct, δ^* is the same for each surface, since the velocity profile is symmetric.

The ejection-rate parameter $Re_{d,w}$, which is used in tables I and II, is converted by introducing δ^* and u_m. This procedure yields

$$Re_{d,w} = \frac{v_w}{u_m} \frac{h}{\delta^*} \frac{u_m \delta^*}{\nu} = \frac{v_w}{u_m} \frac{h}{\delta^*} Re_{\delta^*} \tag{26}$$

The parameter corresponding to equation (15) is

$$\Phi_2 = \frac{\delta^*}{h} Re_{d,w} \tag{27}$$

The pressure drop in channel flow is determined by equation (11). Introducing δ^* and u_m into this relation results in

$$Re_{\delta^*} \frac{\delta^* \frac{\partial p}{\partial x}}{\rho u_m^2} \frac{u_m}{\bar{u}} \left(\frac{h}{\delta^*}\right)^2 = 4A_2 \tag{28}$$

The parameter corresponding to equation (16) is, therefore,

$$\Pi_{2,x} = 4 \frac{\bar{u}}{u_m} \left(\frac{\delta^*}{h}\right)^2 A_2 = \frac{4}{f'_{2,m}} \left(\frac{\delta^*}{h}\right)^2 A_2 \tag{29}$$

The wall shear stress is given by equation (13). Replacing the length x by δ^* results in

$$f''_{2,w} = \frac{\tau_w}{\rho u_m^2} \frac{h}{\delta^*} \frac{u_m}{\bar{u}} \frac{Re_{\delta^*}}{2} \tag{30}$$

From this, the friction parameter

$$T_2 = -\frac{4f''_{2,w}}{f'_{2,m}} \frac{\delta^*}{h} \tag{31}$$

which corresponds to equation (17) is obtained. The minus sign arises from the fact that y_1 was measured in a direction opposite to the one used for boundary-layer flow. The parameters δ^*/h, Φ_2, $\Pi_{x,2}$, and T_2 are calculable from information in table I.

Semiporous duct. - The semiporous duct has a different δ^* for flow along the solid and the porous surface, since u_m generally is not at the center of the duct.

The pressure drop and wall-shear-stress parameters for the semiporous duct are given by equations (11a) and (13a). The parameters corresponding to equations (15), (16), and (17) may be obtained from these relations and the definition of $Re_{d,w}$ in the same manner as for the fully porous channel:

$$\left.\begin{aligned} \Phi_{1,s} &= \left(\frac{\delta^*}{h}\right)_s Re_{d,w,s} \\ \Phi_{1,p} &= \left(\frac{\delta^*}{h}\right)_p Re_{d,w,p} \end{aligned}\right\} \tag{32}$$

$$\left.\begin{aligned} \Pi_{1,x,s} &= \frac{\bar{u}}{u_m}\left(\frac{\delta^*}{h}\right)_s^2 A_1 = \frac{1}{f'_{1,m}}\left(\frac{\delta^*}{h}\right)_s^2 A_1 \\ \Pi_{1,x,p} &= \frac{\bar{u}}{u_m}\left(\frac{\delta^*}{h}\right)_p^2 A_1 = \frac{1}{f'_{1,m}}\left(\frac{\delta^*}{h}\right)_p^2 A_1 \end{aligned}\right\} \tag{33}$$

$$\left.\begin{aligned} T_{1,s} &= +\frac{2f''_{1,w,s}}{f'_{1,m}}\left(\frac{\delta^*}{h}\right)_s \\ T_{1,p} &= -\frac{2f''_{1,w,p}}{f'_{1,m}}\left(\frac{\delta^*}{h}\right)_p \end{aligned}\right\} \tag{34}$$

The sign in the equation for T is governed by the direction in which y is measured. The preceding parameters may be calculated from values in table II and are given in table V.

4518

Porous tube. - An investigation to determine how δ^* should be defined so as to correspond best to the boundary-layer-displacement thickness showed that the tube-flow parameters agreed best with those for the other geometries when equation (25) was used with y interpreted as the radial distance from the tube wall (y_w becomes equal to R).

The ejection rate is expressed in table III by the parameter $Re_{t,w}$. Introducing δ^* and u_m results in

$$Re_{t,w} = \frac{v_w}{u_m}\frac{u_m\delta^*}{\nu}\frac{R}{\delta^*} = \frac{v_w}{u_m}\frac{R}{\delta^*}Re_{\delta^*} \tag{35}$$

and the parameter corresponding to equation (15) is

$$\Phi_t = \frac{\delta^*}{R}Re_{t,w} \tag{36}$$

The characteristic parameter for the pressure drop is given by equation (11b). Introducing δ^* and u_m results in

$$Re_{\delta^*}\frac{\delta^*\frac{\partial p}{\partial x}}{\rho u_m^2}\frac{u_m}{\bar{u}}\left(\frac{R}{\delta^*}\right)^2 = 8A_t \tag{37}$$

By using equations (37) and (9b) and dividing by 2, the pressure-drop parameter Π_x (eq. (16)) becomes

$$\Pi_{t,x} = \frac{2A_t}{f'_{t,m}}\left(\frac{\delta^*}{R}\right)^2 \tag{38}$$

where the division by 2 matches $\Pi_{t,x}$ with $\Pi_{d,x}$ for impermeable walls: $\Pi_{t,x} = \Pi_{d,x}$ when $Re_w = 0$.

From equation (13b) the parameter for the wall shear stress

$$T_t = -4 \frac{f''_{t,w}}{f'_{t,m}} \frac{\delta^*}{R} \tag{39}$$

4518 which corresponds to equation (17) is obtained. These parameters may be calculated from table III and are given in table V.

COMPARISON OF FLOW CHARACTERISTICS FOR BOUNDARY-LAYER AND CHANNEL FLOW

CY-3 Figures 3 to 5 present the results of calculations that converted the various parameters used in the section SOLUTION OF THE DIFFERENTIAL EQUATIONS to the ones developed in the section COMMON PARAMETERS FOR BOUNDARY-LAYER AND CHANNEL FLOW. Table V presents a summary of the dimensionless parameters for different geometries.

Pressure Gradient

The ejection-rate parameter Φ is used as the abscissa in figure 3 because it has to be considered as the independent variable for boundary-layer as well as for channel flow. The situation is different with regard to the pressure-drop parameter Π_x. The pressure drop is an independent variable for boundary-layer flow impressed on the boundary layer by the main stream. Correspondingly, a series of dashed curves using the Euler number as parameter represents the boundary-layer flow in figure 3. For channel flow, however, the pressure drop is uniquely determined by the ejection-rate parameter, and only one curve appears in figure 3 for each geometry representing the duct with two porous walls, the duct with one porous wall (considering the porous surface), and the tube.

A comparison of the curves for the various duct geometries (fig. 3(b)) reveals that the two curves for the ducts with one and two porous walls are quite close together. This proximity indicates that, for these duct-flow geometries, the pressure-drop parameter is almost the same function of the ejection-rate parameter. For boundary-layer flow, a certain value of the Euler number that makes the pressure-drop parameter equal to the one for duct flow exists for each ejection rate. For the solid surface $\Phi = 0$, this Euler number has a value of approximately 0.12. This value increases with increasing ejection rate and has, for instance, at

$\Phi = -2.0$ a value of approximately 0.4 for the semiporous duct, 0.2 for the tube, and 0.5 for the fully porous duct, as may be interpreted from figure 3(b). Too little information is available for suction on the various geometries to make a detailed comparison, but, in a qualitative way, the difference for the various geometries appears to be larger in this range.

Shear Stress

The shear parameter T plotted over the ejection-rate parameter is presented in figure 4. A series of dashed curves with the Euler number as parameter again represents boundary-layer flow, and channel flow is shown by single curves for each of the various geometries. In the suction range, no agreement exists between the various channel flows, even in a qualitative way. The curves for the ducts with one and two porous walls again agree quite well with each other in the ejection range; the values for tube flow are somewhat higher. The shear-stress parameter for zero ejection is identical for all channel geometries. Again, an Euler number that makes the shear parameter for boundary-layer flow agree with the values for the various channel flows can be determined for each ejection rate (e.g., at $\Phi = -2.0$, $Eu = 0.3$ for the semiporous duct, $Eu = 0.45$ for the fully porous duct, and $Eu > 1$ for the tube). 4518

An inspection of figures 3(b) and 4 reveals that, for the two duct flows, the Euler numbers obtained in this way are in extremely good agreement. Thus, the friction parameters for duct flow and boundary-layer flow are almost identical when the proper pressure gradient is chosen for the boundary layer. The agreement is less good between the tube flow and the boundary-layer flow. A comparison of figures 3(b) and 4 also reveals that in both ducts a slight suction corresponding to approximately $\Phi = 0.5$ makes the pressure gradient vanish. The friction parameter agrees very well with the one on a flat plate with constant velocity outside the boundary layer. The agreement is slightly less for the fully porous duct than for the semiporous one.

The shear-stress parameter was also calculated for the solid wall of the duct with parallel walls. With fluid ejection at the porous wall, the shear-stress parameter for the solid wall (not shown in fig. 4) takes on values between 1.33 and 1.47, which are not too far from the value of 1.33 that is valid for all channel geometries and for zero ejection rate (fig. 4). Table V(b) presents these shear-stress parameters for the solid surface as a function of ejection or suction rate.

Velocity Profiles

In order to make a valid comparison of the velocity profiles, a pressure-drop parameter was selected so that profiles were available for

each geometry with a pressure-drop parameter close to the selected one. Figure 5 plots these profiles as the velocity ratio u/u_m over the dimensionless wall distance y/δ^*. The velocity profile for boundary-layer flow was selected as that with an Euler number closest to the value that would make the pressure-drop parameter of the boundary layer agree with that of the channel.

The data of figure 5(a) are valid at zero ejection. In this case the velocity profiles for all channel flows become identical in shape, and the boundary-layer profile agrees quite closely with the channel profiles. The agreement would be even better if a boundary-layer profile for a pressure-drop parameter of -0.222 had been used for the comparison; such a solution, however, is not available. Figures 5(b) and (c) show increasing blowing rates, and figure 5(d) gives ejection rates that bring the pressure-drop parameter close to zero. The various velocity profiles in each figure agree very well with each other, and the differences from one figure to the next also are remarkably small. Certain characteristic trends exist for the various geometries. The tube-flow profile at higher ejection rates is, for instance, fuller than the channel or the boundary-layer profiles. This fullness also is reflected in the fact that the shear-stress parameter for tube flow is higher than for the channel flows. The boundary-layer profiles, on the other hand, approach the value $u/u_m = 1$ more gradually than the channel-flow profiles.

Generally, the characteristics of two-dimensional laminar flow, as indicated by the dimensionless shear-stress parameter and by the shape of the velocity profiles, appear to be determined mainly by the ejection rate and by the pressure drop in the flow. Whether the flow is unconfined as in boundary layers or confined as in a duct is of minor importance. The curvature of the bounding walls of the channel (i.e., whether the channel is a tube or a duct) has a greater influence as can be seen from a comparison of duct or boundary-layer flow with tube flow. For larger ejection rates, even the influence of the ejection parameter on the shear parameter and on the profile shape becomes quite small.

Applications

There are several areas of research in which these findings should be useful, for instance, the development of a procedure based on the momentum integral equation and on the velocity profile shape established in figures 5 and 6. Such a procedure should allow accurate calculations of the flow in porous channels and over porous surfaces both with fluid ejection and with the proper pressure gradient. These boundary-layer and channel-flow relations should also be helpful in deciding what information on boundary-layer flow can be obtained from experiments in channels that are more amenable to experiment (ref. 15). In this connection, the

4518

CY-3 back

influence of surface roughness and pore size (encountered in a fabricated porous wall) is still an open question. It has been seen that, in a duct with constant cross-sectional area in flow direction, only one of the two parameters Φ and Π_x can be adjusted at will. However, when the duct is designed in such a way that the cross-sectional area can be made to increase or decrease in flow direction, any pressure gradient corresponding to a desired Euler number can be produced.

CONCLUSIONS

4518

Solutions of the equations describing laminar steady flow through a duct consisting of two parallel walls, flow through a tube with circular cross section, and boundary-layer flow over a wedge with fluid ejection and suction through the porous walls point out the following facts:

1. Common dimensionless parameters can be developed for all investigated geometries by using a properly defined displacement thickness as the reference length and the maximum velocity as the reference velocity.

2. Comparison of the various flow geometries on the basis of these parameters indicated that the local flow conditions (velocity profile - friction factor) depend primarily on the local pressure-drop and fluid-ejection rates.

3. Under the conditions existing when both the pressure-drop and fluid-ejection-rate parameters are matched for the different geometries:

(a) The confinement of the flow in a duct, or freedom in a boundary layer, influences the flow only to a minor degree.

(b) Curvature of the surface normal to the flow direction has a stronger effect on the flow than the effect of the factor listed under (a), but not as strong as the effect of the local pressure-drop and fluid-ejection rates.

4. The flow parameters for the condition where fluid is sucked away from the stream through the porous surfaces cannot be investigated in the same way as for fluid ejection because of insufficient information. Qualitatively, the influence of the specific geometry on flow characteristics appears to be stronger in suction than in ejection.

Lewis Flight Propulsion Laboratory
National Advisory Committee for Aeronautics
Cleveland, Ohio, September 3, 1957

APPENDIX A

SYMBOLS

A	constant of integration (eqs. (5), (5a), (5b))
a,b,c	arbitrary exponents
B	dimensionless displacement thickness, $\delta^*\sqrt{Re_x}/x$
C_w	friction coefficient, $\dfrac{\tau_w}{\frac{1}{2}\rho u_m^2}$
Eu	Euler number $\dfrac{-x\partial p/\partial x}{\rho u_m^2}$, $u_m = \text{const.}\ (x^{Eu})$
f	dimensionless stream function
f',f'',f'''	first, second, and third derivatives of f with respect to η
h	channel height (shown in figs. 1(a) and (b))
K	interpolation constant (eqs. (C4))
p	static pressure
R	radius of tube
r	distance in normal flow direction for tube
Re_1	main-flow Reynolds number using average velocity for semiporous duct, $2\overline{u}(x)h/\nu$
Re_2	main-flow Reynolds number using average velocity for fully porous duct, $2\overline{u}(x)h/\nu$
Re_t	main-flow Reynolds number using average velocity for porous tube, $2\overline{u}(x)R/\nu$
$Re_{1,0}$	main-flow Reynolds number using average inlet velocity for semiporous duct, $2\overline{u}(0)h/\nu$
$Re_{2,0}$	main-flow Reynolds number using average inlet velocity for fully porous duct, $2\overline{u}(0)h/\nu$

$Re_{t,0}$	main-flow Reynolds number using average inlet velocity for porous tube, $2\overline{u}(0)R/\nu$
$Re_{d,w}$	wall Reynolds number for porous duct, $v_w h/\nu$
$Re_{t,w}$	wall Reynolds number for porous tube, $v_w R/\nu$
$Re_{b,x}$	main-flow Reynolds number for wedge flow, $u_m x/\nu$
Re_{δ^*}	displacement Reynolds number, $u_m \delta^*/\nu$
u	fluid velocity parallel to wall
v	fluid velocity normal to wall
x	distance in main-flow direction
y	distance in normal flow direction for all geometries except the tube (see r)
β	parameter $\frac{2Eu}{Eu + 1}$
δ^*	displacement thickness in channel or tube, $\int_0^{y_m} \left(1 - \frac{u}{u_m}\right) dy$
δ_b^*	boundary-layer displacement thickness, $\int_0^{\infty} \left(1 - \frac{u}{u_m}\right) dy$
η_b	dimensionless normal distance for wedge flow, $y\sqrt{u_m/\nu x}$
η_t	dimensionless normal distance for porous tube, $(r/R)^2$
η_1	dimensionless normal distance for semiporous duct, y/h
η_2	dimensionless normal distance for fully porous duct, $2y/h$
μ	viscosity of fluid
ν	kinematic viscosity of fluid, μ/ρ
Π_x	pressure-gradient parameter, $Re_{\delta^*} \frac{\delta^* \partial p/\partial x}{\rho u_m^2}$
ρ	density of fluid

T	wall friction parameter, $Re_{\delta^*} \frac{\tau_w}{\frac{1}{2}\rho u_m^2}$
τ_w	wall shear stress, $\mu(\partial u/\partial y)_w$
$\tau_{1,w}$	wall shear stress for semiporous duct, $\mu\bar{u}(x)f''_{1,w}/h$
$\tau_{2,w}$	wall shear stress for fully porous duct, $2\mu\bar{u}(x)f''_{2,w}/h$
$\tau_{b,w}$	wall shear stress for wedge flow, $\mu u_m\sqrt{Re_x}f''_{b,w}/x$
$\tau_{t,w}$	wall shear stress for porous tube, $2\mu\bar{u}(x)f''_{t,w}/R$
Φ	flow parameter, $\frac{v_w}{u_m} Re_{\delta^*}$
ψ	stream function
ψ_1	stream function for semiporous duct, $h\bar{u}(x)f_1$
ψ_2	stream function for fully porous duct, $\frac{h}{2}\bar{u}(x)f_2$
ψ_b	stream function for wedge flow, $\sqrt{\nu x u_m}\, f_b$
ψ_t	stream function for porous tube, $R^2\bar{u}(x)f_t$

Subscripts:

b	boundary layer or wedge
d	duct
m	maximum
p	porous wall
s	solid wall
t	porous tube
w	wall
x	x-direction

1	semiporous duct
2	fully porous duct
I,II	trial number
∞	main stream outside boundary layer

Superscripts:

$\bar{}$	average value
$\sim$	denotes transformed dimensionless quantities (appendix B)

4518

CY-4

APPENDIX B

COMPARISON OF RESULTS WITH PREVIOUS INVESTIGATIONS

The following table compares the results of the present numerical integrating techniques (five-point or Runge-Kutta formula) with those of other techniques and with perturbation solutions. The comparison is made for the fully porous duct and for the porous tube. The integration constant A and the first and second derivatives of the tabulated function f, f'(0) and f"(1), are given for different values of the wall Reynolds number Re_w for the fully porous duct and for the porous tube. As noted by equations (9) and (13), f'(0) and f"(1) are related to the ratio of maximum to average velocity and to the shear stress, respectively.

(a) Fully porous duct

Investigator	Reference	A_2	$f_2'(0)$	$f_2''(1)$
$Re_{d,w} = -20$				
Yuan[a]	16	-26.723	1.51365	-2.6756
Berman	17		1.538	
(b)	--	-27.0284	1.5380	-2.6382
$Re_{d,w} = 2$				
(a)	4	-0.7031	1.4923	-3.095
(b)	--	-.7046	1.4923	-3.0964
$Re_{d,w} = 40$				
Sellars[a]	18	18.8916	1.0554	-21.108
Yuan[a]	16	47.299	1.5994	-2.3634
Berman	17		1.150	
(b)	--	26.054991	1.1550783	-15.7047
(c)	--	26.054991	1.1550783	-15.7129
$Re_{d,w} = 98$				
Sellars[a]	18	47.958	1.0213	-50.042
Yuan[a]	16	118.853	1.5824	-2.4249
(b)	--	53.313961	1.0430000	-16.7769
(b)	--	53.313962	1.0430000	94.4472
(c)	--	53.313961	1.0430000	-16.9776

(b) Porous tube

Investigator	Reference	A_t	$f_t'(0)$	$f_t''(1)$
$Re_{t,w} = -10$				
Yuan[a]	5	-7.4938	0.8698	-1.2520
(b)	--	-7.4752	..8467	-1.2052
$Re_{t,w} = -2$				
Yuan[a]	5	-2.3370	0.9504	-1.0704
(b)	--	-2.3980	.9278	-1.1054
$Re_{t,w} = 1$				
Yuan[a]	5	-0.20926	1.0709	-0.8926
(b)	--	-.19095	1.0777	-.8823
$Re_{t,w} = 2$				
Yuan[a]	5	0.6630	1.1726	-0.7370
(b)	--	.9807	1.2907	-.5633

[a]Perturbation solution.

[b]Present report, five-point formula.

[c]Present report, Runge-Kutta formula.

The results given for references 4, 5 and 16 (Yuan), and 18 (Sellars) are calculated from equations obtained in the perturbation analyses performed therein. The reference 17 results (Berman) are taken from a curve given in that report, which gives values only for the ratio of the maximum to the average axial velocity for a series of ejection and suction parameter values.

The table shows that the results for the fully porous duct at both $Re_{d,w} = -20$ and 2 agree well. As noted in reference 4, accurate perturbation solutions are limited to small values of Re_w when the solution is perturbed about $Re_w = 0$. Similar reasoning holds for perturbation solutions obtained for large values of Re_w; that is, as Re_w takes on smaller values, such a solution becomes less accurate. Although Sellars (ref. 18) noted that his approach may not be good unless $Re_{d,w} \approx 100$, a value is included at $Re_{d,w} = 40$ for comparison purposes. At both $Re_{d,w} = 40$ and 98, the results of reference 16 are much higher than those of the other studies.

For the porous tube, the perturbation solution of Yuan (ref. 16) at $Re_{t,w} = 10$ yields good values not only for A_t and $f_t'(0)$ but also for $f_t''(1)$ (and, hence, friction, eq. (13b)). At the smaller values of $Re_{t,w}$, the agreement is fair at ± 2 but improves as $Re_{t,w}$ approaches 0 (e.g., 1).

APPENDIX C

MODIFICATIONS REQUIRED AND EFFECT OF STEP SIZE IN NUMERICAL SOLUTIONS

Duct

Since finding a solution of equation (5) for a large Reynolds number $Re_{d,w}$ (>40) proved difficult, the following transformation was made:

Let

$$\eta_2 \equiv \left(\frac{Re_{d,w}}{2}\right)^{-a} \tilde{\eta}_2, \quad \tilde{f}_2 \equiv \left(\frac{Re_{d,w}}{2}\right)^{b} \tilde{f}_2, \text{ and } A_2 \equiv \left(\frac{Re_{d,w}}{2}\right)^{c} \tilde{A}_2$$

Substitution for f_2, η_2, and A_2 in equation (5) gives

$$\left(\frac{Re_{d,w}}{2}\right)^{2a+2b+1}\left(\tilde{f}_2\tilde{f}_2'' - \tilde{f}_2'^2\right) + \left(\frac{Re_{d,w}}{2}\right)^{c} \tilde{A}_2 = \left(\frac{Re_{d,w}}{2}\right)^{3a+b} \tilde{f}_2''' \tag{C1}$$

By choosing a, b, and c properly, the important terms in the differential equation can then be made the same order in $Re_{d,w}$ (ref. 14, p. 11). Thus, if $a = 1/2$, $b = -1/2$, and $c = 1$, equation (C1) reduces to

$$\tilde{f}_2\tilde{f}_2'' - \tilde{f}_2'^2 + \tilde{A}_2 = \tilde{f}_2''' \tag{C2}$$

where

$$\tilde{f}_2 = (Re_{d,w}/2)^{1/2} f_2$$

$$\tilde{f}_2 = \tilde{f}_2'$$

$$\tilde{f}_2'' = (Re_{d,w}/2)^{-1/2} f_2''$$

The boundary conditions associated with equation (C2) are then

$$\left.\begin{aligned} &\eta_2 = 0;\ \tilde{\eta}_2 = 0;\ \tilde{f}_2 = 0;\ \tilde{f}_2'' = 0 \\ &\eta_2 = 1;\ \tilde{\eta}_2 = (Re_{d,w}/2)^{1/2};\ \tilde{f}_2 = (Re_{d,w}/2)^{1/2};\ \tilde{f}_2' = 0 \end{aligned}\right\} \tag{C3}$$

Equation (C2) was solved for $Re_{d,w} = 98$ on the IBM 650 computer by using the Runge-Kutta integrating method. The results are listed in table I(j). This solution was then checked in the original total differential equation (5b) by using the five-point integration formulas. Results are shown in table I(h) and (i). In this particular case eight significant figures were not sufficient to satisfy the boundary conditions. The change caused by a difference of one in the eighth significant figure can be seen in table I(h) and (i). A technique similar to that discussed later for boundary-layer flow possibly could be used by starting at $\eta \sim 0.5$. The Sellars solution of reference 18 also should be useful in this region. 4518

Tube

For the porous tube, two solutions were found at $Re_{t,w} = 2$ and at $Re_{t,w} = 10$. Of the two solutions for $Re_{t,w} = 2$, the one listed in table III(e) ($A_t = 0.9087$ and $f_t''(1) = -0.5633$) appears to fit better with an extrapolation of the curve determined by the solutions for other $Re_{t,w}$ values (fig. 7). The two solutions for $Re_{t,w} = 10$ are far away from any reasonable extrapolation of the curve obtained from the other solutions, and u_m is not at the center of the channel, as may be seen from a study of table III(g) and (h). Although a considerable amount of effort was expended, solutions to equation (5b) satisfying equation (6b) for $2 < Re_{t,w} < 10$ were not found. A possible explanation for the lack of solutions in this range follows.

A pressure rise in main-flow direction is connected with the fluid suction in channel flow when Re_w is sufficiently high. (The pressure increases in flow direction when A is positive, cf. eqs. (11).) The lack of solutions for the intermediate suction rates ($2 < Re_{t,w} < 10$) may be analogous to the difficulty encountered by Hartree (ref. 19) in solving the boundary-layer equation near the separation point, which is defined as the solution of the boundary-layer equation where $f_b''(0) = 0$ or $\tau_{b,w} = 0$ (eq. (13c)). In the porous-tube calculation, $f_t''(1)$ is close to zero for $Re_{t,w} > 2$ (see fig. 7).

Similar trouble was encountered in the semiporous duct for $Re_{d,w} > 13$. As may be seen in table II(e), (f), and (g), $f_1''(0)$ is approaching zero in this region; that is, because of the suction at the porous wall, the fluid is pulled away from the solid wall, and the shear stress at the solid wall tends toward zero as separation at the solid wall is imminent. No such difficulty was experienced for the fully porous duct and, for all values of $Re_{d,w}$, $f_2''(1)$ was far from zero (table I(a), (b), and (c)).

In the geometries where a numerical solution was difficult, therefore, the values of Re_w are such that the wall shear stress is close to zero. This instability for channel flow possibly is analogous to that discussed in reference 19 for separated boundary-layer flow. If desired, Re_w could be found such that $f_d''(1)$ or $f_t''(1) = 0$, which would be analogous to Hartree's finding of $\beta = -0.1988$, yielding $f_b''(0) = 0$ (ref. 19). Such a calculation was not pursued.

Attempts were made without success to find additional solutions of equation (5b) for $Re_{t,w} < 0$. No attempt was made to find an additional solution for $Re_{t,w} = 1$.

Boundary Layer

A few solutions in addition to those in references 13, 20, 21, 22, and 23 for the wedge flow were obtained in a similar manner by using punched cards on the IBM Card-Programmed Calculator. (These solutions were found shortly after publication of ref. 13, at which time an IBM 650 computer was not available.) In these solutions (table IV), eight significant figures for $f_b''(0)$ were not sufficient to satisfy the boundary condition $f_b'(\infty) = 1$. In fact, one $f_b'(\eta)$ curve went above the prescribed $f'(\infty)$ condition and the other (having a $f_b''(0)$ value that differed by only one in the eighth significant figure) went below it (fig. 6). The method devised for interpolating between these two near-solutions consisted of using, as a starting point for the final integration, interpolated values at some intermediate point (say $\eta_b = 4$) where the differences between solutions are in, perhaps, the sixth place. Sample equations for the new starting values are

$$\left.\begin{aligned}
f_b &= Kf_{b,I} + (1 - K)\, f_{b,II} \quad \text{at} \quad \eta_b = 4 \\
f_b' &= Kf_{b,I}' + (1 - K)\, f_{b,II}' \quad \text{at} \quad \eta_b = 4 \\
f_b'' &= Kf_{b,I}'' + (1 - K)\, f_{b,II}'' \quad \text{at} \quad \eta_b = 4 \\
f_b''' &= Kf_{b,I}''' + (1 - K)\, f_{b,II}''' \quad \text{at} \quad \eta_b = 4
\end{aligned}\right\} \tag{C4}$$

By proper choice of K, the desired condition on $f_b'(\infty)$ can be approximated closely enough. The effective $f_b''(0)$ would then be $Kf_{b,I}''(0) + (1 - K)\, f_{b,II}''(0)$, a number with more than eight significant figures. Table IV gives only the interpolated values.

4518

Effect of Step Size on Solution

A step-size check was made at the extreme wall Reynolds number for each of the channel geometries. In most cases, a step-size $\Delta\eta = 0.025$ was sufficiently small. The following table shows the results of these step-size checks:

(a) Fully porous duct

$Re_{d,w}$	$f_2'(0)$	A_2	$\Delta\eta_2$	$f_2(1)$	$f_2'(1)$	$f_2''(1)$	$f_2'''(1)$
-20	1.5380	-27.0284	0.05	1.0000	0.000011	-2.6393	-0.6356
-20	1.5380	-27.0284	.025	1.0000	.000001	-2.6382	-.6464
20	1.3549	16.4780	.025	1.0000	.000005	-5.9974	-43.496
20	1.3549	16.4770	.01	1.0000	.000003	-5.9989	-43.512
98	1.0430000	53.313961	.01	.7646	11.9381	-16.7769	-30037.447
98	1.0430000	53.313962	.01	1.2669	11.3912	94.4472	24386.718
98	1.0430002	53.313962	.005	.6461	-17.4837	-882.4353	-42863.032
98	1.0430003	53.313962	.005	1.4064	17.9747	814.7355	40368.260

(b) Semiporous duct

$Re_{d,w}$	$f_1''(0)$	A_1	$\Delta\eta_1$	$f_1(1)$	$f_1'(1)$	$f_1''(1)$	$f_1'''(1)$
-20	13.0038	-65.3486	0.025	0.9999	-0.0002	-3.1067	-3.2192
-20	13.0040	-65.0040	.01	1.0000	-.0001	-3.2420	-.5100
-20	13.0039	-65.3486	.0025	1.0000	.0000	-3.2418	-.5126
13	.0855	9.1350	.025	1.0000	.0000	-30.283	-384.54
13	.0832	9.1406	.01	1.0000	.0000	-30.321	-385.04

(c) Porous tube

$Re_{t,w}$	$f_t''(1)$	A_t	$\Delta\eta_t$	$f_t(0)$	$f_t'(0)$	$f_t''(0)$	$\eta_t f_t'''(0)$
-10	-1.2052	-7.4750	0.05	0.000003	0.8466	-0.3116	0.0043
-10	-1.2052	-7.4752	.025	-.000004	.8467	-.3158	.0093
10	-2.2940	3.3059	.05	.000000	.4907	.8979	.0000
10	-2.2940	3.3058	.025	.00000	.4907	.8980	.0000

Step-size checks were also made for intermediate wall Reynolds numbers. However, the greatest differences due to step size were at the extreme wall Reynolds numbers; these are shown in the preceding tables.

A study of the table for the fully porous duct shows that the values of f_2 and its derivatives at $\eta = 1$ for $Re_{d,w} = 98$ are considerably different for $\Delta\eta = 0.01$ and $\Delta\eta = 0.005$. Since the input values ($f_2'(0)$ and A_2) changed very little, solutions at a smaller step size were not attempted.

REFERENCES

1. Livingood, John N. B., and Donoughe, Patrick L.: Summary of Laminar-Boundary-Layer Solutions for Wedge-Type Flow over Convection- and Transpiration-Cooled Surfaces. NACA TN 3588, 1955.

2. Berman, Abraham S.: Laminar Flow in Channels with Porous Walls. Jour. Appl. Phys., vol. 24, no. 9, Sept. 1953, pp. 1232-1235.

3. Berman, Abraham S.: Laminar Flow in Channels with Porous Walls. Rep. No. K-944, Carbide and Carbon Chem. Co., Oak Ridge (Tenn.), Nov. 28, 1952. (U.S. Govt. Contract W-7405-eng-26.)

4. Donoughe, Patrick L.: Analysis of Laminar Incompressible Flow in Semiporous Channels. NACA TN 3759, 1956.

5. Yuan, S. W., and Finkelstein, A. B.: Laminar Pipe Flow with Injection and Suction Through a Porous Wall. Trans. ASME, vol. 78, no. 4, May 1956, pp. 719-724.

6. Rubesin, Morris W.: An Analytical Estimation of the Effect of Transpiration Cooling on the Heat-Transfer and Skin-Friction Characteristics of a Compressible Turbulent Boundary Layer. NACA TN 3341, 1954.

7. Dorrance, William H., and Dore, Frank J.: The Effect of Mass Transfer on the Compressible Turbulent Boundary-Layer Skin Friction and Heat Transfer. Jour. Aero. Sci., vol. 21, no. 6, June 1954, pp. 404-410.

8. Dorrance, William H.: The Effect of Mass Transfer on the Compressible Turbulent Boundary-Layer Skin Friction and Heat Transfer - An Addendum. Jour. Aero. Sci., vol. 23, no. 3, Mar. 1956, pp. 283-284.

9. Rannie, W. D.: A Simplified Theory of Porous Wall Cooling. Prog. Rep. 4-50, Power Plant Lab., Jet Prop. Lab., C.I.T., Nov. 24, 1947. (AMC Contract W-535-ac-20260, Ord. Dept. Contract W-04-200-ORD-455.)

10. Weissberg, Harold L., and Berman, Abraham S.: Velocity and Pressure Distributions in Turbulent Pipe Flow with Uniform Wall Suction. Ch. XIV of Heat Transfer and Fluid Mech. Inst., Los Angeles (Calif.), 1955.

11. Weissberg, Harold L.: Velocity and Pressure Distributions in Turbulent Pipe Flow with Uniform Wall Suction. Rep. No. K-1187, Carbide and Carbon Chem. Co., Oak Ridge (Tenn.), Mar. 29, 1955.

12. Schlichting, Hermann: Boundary Layer Theory. McGraw-Hill Book Co., Inc., 1955.

13. Donoughe, Patrick L., and Livingood, John N. B.: Exact Solutions of Laminar-Boundary-Layer Equations with Constant Property Values for Porous Wall with Variable Temperature. NACA Rep. 1229, 1955. (Supersedes NACA TN 3151.)

14. Ostrach, Simon: An Analysis of Laminar Free-Convection Flow and Heat Transfer About a Flat Plate Parallel to the Direction of the Generating Body Force. NACA Rep. 1111, 1953. (Supersedes NACA TN 2635.)

15. Eckert, E. R. G., Diaguila, Anthony J., and Donoughe, Patrick L.: Experiments on Turbulent Flow Through Channels Having Rough Surfaces with or without Air Injection. NACA TN 3339, 1955.

16. Yuan, S. W.: Further Investigation of Laminar Flow in Channels with Porous Walls. Jour. Appl. Phys., vol. 27, no. 3, Mar. 1956, pp. 267-269.

17. Berman, Abraham S.: Concerning Laminar Flow in Channels with Porous Walls. Jour. Appl. Phys., vol. 27, no. 12, Dec. 1956, pp. 1557-1558.

18. Sellars, John R.: Laminar Flow in Channels with Porous Walls at High Suction Reynolds numbers. Jour. Appl. Phys., vol. 26, no. 4, Apr. 1955, pp. 489-490.

19. Hartree, D. R.: On an Equation Occurring in Falkner and Skan's Approximate Treatment of the Equations of the Boundary Layer. Proc. Cambridge Phil. Soc., vol. 33, pt. 2, Apr. 1937, pp. 223-239.

20. Brown, W. Byron, and Donoughe, Patrick L.: Tables of Exact Laminar-Boundary-Layer Solutions When the Wall is Porous and Fluid Properties are Variable. NACA TN 2479, 1951.

21. Emmons, H. W., and Leigh, D.: Tabulation of the Blasius Function with Blowing and Suction. Interim Tech. Rep. No. 9, Combustion Aero. Lab., Div. Appl. Sci., Harvard Univ., Nov. 1953. (Army Ord. Dept. Contract No. DA-19-020-ORD-1029.)

22. Schaefer, H.: Laminare Grenzschicht mit Absaugung und Ausblasen in der Potentialströmung $U = U_1 \cdot X^m$. UM 2043, Deutsche Luftfahrtforschung, 1944.

23. Schlichting, Hermann, and Bussman, Karl: Exakte Lösungen für die laminare Grenzschicht mit Absaugung und Ausblasen. Schriften d.D. Akad. Luftfahrtforschung, Bd. 7B, Heft 2, 1953.

24. Tetervin, Neal: A Study of the Stability of the Incompressible Laminar Boundary of Infinite Wedges. NACA TN 2976, 1953.

4518

CY-5

TABLE I. - NUMERICAL SOLUTIONS FOR FULLY POROUS DUCT

(a) $Re_{d,w} = -20$ (ejection) $A_2 = -27.0284$
$f_2'(0) = 1.5380$ $\delta^*/h = 0.17489$

η_2	f_2	f_2'	f_2''	f_2'''
0.00	0.0000	1.5380	0.0000	-3.3751
.05	.0768	1.5337	-.1688	-3.3751
.10	.1532	1.5211	-.3375	-3.3742
.15	.2288	1.5000	-.5061	-3.3705
.20	.3031	1.4705	-.6744	-3.3611
.25	.3757	1.4326	-.8421	-3.3423
.30	.4462	1.3863	-1.0085	-3.3105
.35	.5148	1.3317	-1.1729	-3.2621
.40	.5792	1.2691	-1.3343	-3.1942
.45	.6410	1.1984	-1.4919	-3.1046
.50	.6990	1.1199	-1.6444	-2.9918
.55	.7528	1.0340	-1.7907	-2.8550
.60	.8022	.9410	-1.9295	-2.6941
.65	.8468	.8412	-2.0597	-2.5095
.70	.8863	.7352	-2.1801	-2.3020
.75	.9202	.6234	-2.2895	-2.0726
.80	.9485	.5064	-2.3870	-1.8225
.85	.9708	.3849	-2.4715	-1.5533
.90	.9869	.2595	-2.5420	-1.2664
.95	.9967	.1310	-2.5978	-.9637
1.00	1.0000	.0000	-2.6382	-.6468

(b) $Re_{d,w} = -10$ (ejection) $A_2 = -14.8704$
$f_2'(0) = 1.5252$ $\delta^*/h = 0.17217$

f_2	f_2'	f_2''	f_2'''	η_2
0.0000	1.5252	0.0000	-3.2394	0.00
.0762	1.5211	-.1620	-3.2394	.05
.1520	1.5090	-.3239	-3.2390	.10
.2270	1.4887	-.4858	-3.2373	.15
.3007	1.4604	-.6476	-3.2327	.20
.3729	1.4240	-.8090	-3.2234	.25
.4430	1.3795	-.9698	-3.2070	.30
.5107	1.3270	-1.1296	-3.1818	.35
.5756	1.2666	-1.2878	-3.1434	.40
.6372	1.1983	-1.4437	-3.0913	.45
.6953	1.1223	-1.5966	-3.0228	.50
.7493	1.0387	-1.7457	-2.9359	.55
.7990	.9478	-1.8899	-2.8290	.60
.8440	.8498	-2.0282	-2.7009	.65
.8839	.7451	-2.1596	-2.5508	.70
.9184	.6340	-2.2829	-2.3780	.75
.9472	.5169	-2.3970	-2.1825	.80
.9700	.3944	-2.5008	-1.9641	.85
.9865	.2671	-2.5930	-1.7233	.90
.9966	.1354	-2.6727	-1.4605	.95
1.0000	.0000	-2.7387	-1.1766	1.00

(c) $Re_{d,w} = -2$ (ejection) $A_2 = -5.3303$
$f_2'(0) = 1.5066$ $\delta^*/h = 0.16814$

η_2	f_2	f_2'	f_2''	f_2'''
0.00	0.0000	1.5066	0.0000	-3.0604
.05	.0753	1.5028	-.1530	-3.0604
.10	.1502	1.4913	-.3060	-3.0603
.15	.2243	1.4722	-.4590	-3.0600
.20	.2972	1.4454	-.6120	-3.0592
.25	.3687	1.4110	-.7649	-3.0574
.30	.4382	1.3689	-.9177	-3.0542
.35	.5055	1.3192	-1.0703	-3.0490
.40	.5700	1.2619	-1.2226	-3.0410
.45	.6315	1.1970	-1.3744	-3.0296
.50	.6896	1.1245	-1.5255	-3.0139
.55	.7438	1.0444	-1.6757	-2.9930
.60	.7939	.9569	-1.8247	-2.9660
.65	.8394	.8620	-1.9722	-2.9318
.70	.8800	.7597	-2.1177	-2.8895
.75	.9153	.6503	-2.2610	-2.8381
.80	.9449	.5337	-2.4014	-2.7765
.85	.9685	.4102	-2.5384	-2.7036
.90	.9858	.2799	-2.6715	-2.6184
.95	.9964	.1431	-2.8000	-2.5199
1.00	1.0000	.0000	-2.9233	-2.4070

(d) $Re_{d,w} = 2$ (suction) $A_2 = -0.7046$
$f_2'(0) = 1.4923$ $\delta^*/h = 0.16494$

f_2	f_2'	f_2''	f_2'''	η_2
0.0000	1.4923	0.0000	-2.9315	0.00
.0746	1.4886	-.1466	-2.9315	.05
.1487	1.4776	-.2932	-2.9316	.10
.2222	1.4593	-.4397	-2.9319	.15
.2945	1.4337	-.5864	-2.9327	.20
.3654	1.4007	-.7330	-2.9344	.25
.4345	1.3603	-.8798	-2.9374	.30
.5013	1.3127	-1.0268	-2.9425	.35
.5656	1.2577	-1.1741	-2.9505	.40
.6270	1.1953	-1.3219	-2.9621	.45
.6850	1.1255	-1.4704	-2.9786	.50
.7394	1.0482	-1.6199	-3.0011	.55
.7897	.9635	-1.7706	-3.0318	.60
.8356	.8711	-1.9231	-3.0705	.65
.8767	.7711	-2.0779	-3.1209	.70
.9126	.6633	-2.2355	-3.1847	.75
.9429	.5475	-2.3966	-3.2642	.80
.9672	.4235	-2.5622	-3.3622	.85
.9851	.2913	-2.7332	-3.4819	.90
.9962	.1501	-2.9108	-3.6269	.95
1.0000	.0000	-3.0964	-3.8009	1.00

TABLE I. - Continued. NUMERICAL SOLUTIONS FOR FULLY POROUS DUCT

(e) $Re_{d,w} = 10$ (suction) $A_2 = 7.9139$
$f_2'(0) = 1.4473$ $\delta^*/h = 0.15453$

η_2	f_2	f_2'	f_2''	f_2'''
0.00	0.0000	1.4473	0.0000	-2.5589
.05	.0723	1.4441	-.1279	-2.5589
.10	.1443	1.4345	-.2559	-2.5591
.15	.2156	1.4185	-.3839	-2.5603
.20	.2860	1.3961	-.5120	-2.5634
.25	.3552	1.3673	-.6403	-2.5702
.30	.4227	1.3320	-.7691	-2.5830
.35	.4882	1.2904	-.8987	-2.6051
.40	.5516	1.2421	-1.0298	-2.6408
.45	.6124	1.1873	-1.1631	-2.6961
.50	.6702	1.1258	-1.2999	-2.7788
.55	.7248	1.0573	-1.4416	-2.8997
.60	.7758	.9815	-1.5907	-3.0731
.65	.8228	.8980	-1.7602	-3.3187
.70	.8655	.8062	-1.9242	-3.6689
.75	.9033	.7053	-2.1187	-4.1421
.80	.9358	.5939	-2.3415	-4.8058
.85	.9625	.4705	-2.6035	-5.7217
.90	.9826	.3326	-2.9194	-6.9828
.95	.9955	.1773	-3.3096	-8.7160
1.00	1.0000	.0000	-3.8017	-11.0946

(f) $Re_{d,w} = 20$ (suction) $A_2 = 16.4780$
$f_2'(0) = 1.3549$ $\delta^*/h = 0.13097$

f_2	f_2'	f_2''	f_2'''	η_2
0.0000	1.3549	0.0000	-1.8800	0.00
.0677	1.3526	-.0940	-1.8800	.05
.1352	1.3458	-.1880	-1.8803	.10
.2022	1.3338	-.2820	-1.8815	.15
.2685	1.3173	-.3762	-1.8850	.20
.3338	1.2961	-.4706	-1.8929	.25
.3980	1.2702	-.5656	-1.9082	.30
.4608	1.2396	-.6616	-1.9359	.35
.5219	1.2040	-.7595	-1.9830	.40
.5811	1.1636	-.8605	-2.0608	.45
.6382	1.1179	-.9664	-2.1864	.50
.6928	1.0668	-1.0803	-2.3869	.55
.7447	1.0097	-1.2070	-2.7055	.60
.7937	.9458	-1.3540	-3.2124	.65
.8392	.8737	-1.5333	-4.0230	.70
.8809	.7916	-1.7644	-5.3300	.75
.9181	.6959	-2.0798	-7.4594	.80
.9501	.5813	-2.5330	-10.9684	.85
.9758	.4388	-3.2150	-16.8191	.90
.9933	.2535	-4.2808	-26.6858	.95
1.0000	.0000	-5.9974	-43.4962	1.00

(g) $Re_{d,w} = 40$ (suction) $A_2 = 26.0550$
$f_2'(0) = 1.1551$ $\delta^*/h = 0.08714$

η_2	f_2	f_2'	f_2''	f_2'''
0.00	0.0000	1.1551	0.0000	-0.6291
.05	.0577	1.1543	-.0315	-.6291
.10	.1154	1.1519	-.0629	-.6292
.15	.1729	1.1480	-.0944	-.6295
.20	.2302	1.1425	-.1259	-.6303
.25	.2871	1.1354	-.1574	-.6323
.30	.3437	1.1267	-.1891	-.6364
.35	.3998	1.1165	-.2211	-.6442
.40	.4553	1.1046	-.2537	-.6590
.45	.5102	1.0911	-.2872	-.6865
.50	.5644	1.0759	-.3227	-.7378
.55	.6178	1.0588	-.3618	-.8352
.60	.6702	1.0396	-.4078	-1.0254
.65	.7217	1.0178	-.4675	-1.4101
.70	.7720	.9924	-.5557	-2.2202
.75	.8208	.9612	-.7053	-4.0020
.80	.8679	.9196	-.9935	-8.1026
.85	.9124	.8565	-1.6090	-17.9804
.90	.9528	.7456	-3.0337	-42.8718
.95	.9851	.5194	-6.5498	-108.3895
1.00	1.0000	.0000	-15.7047	-288.0359

TABLE I. - Concluded. NUMERICAL SOLUTIONS FOR FULLY POROUS DUCT

(h) $Re_{d,w} = 98$ (suction) $\delta^*/h = 0.0206$
$f_2'(0) = 1.0430000$ $f_2'(1) = -11.9381$
$A_2 = 53.313961$

η_2	f_2	f_2'	f_2''	f_2'''
0.00	0.0000	1.0430	0.0000	0.0094
.05	.0522	1.0430	.0005	.0094
.10	.1043	1.0430	.0009	.0094
.15	.1565	1.0431	.0014	.0094
.20	.2086	1.0432	.0019	.0094
.25	.2608	1.0433	.0023	.0094
.30	.3129	1.0434	.0028	.0093
.35	.3651	1.0436	.0033	.0094
.40	.4173	1.0437	.0037	.0093
.45	.4695	1.0439	.0042	.0093
.50	.5217	1.0442	.0047	.0091
.55	.5739	1.0444	.0051	.0083
.60	.6261	1.0447	.0055	.0051
.65	.6784	1.0450	.0054	-.0099
.70	.7306	1.0452	.0035	-.0901
.75	.7829	1.0451	-.0096	-.5784
.80	.8351	1.0431	-.0966	-3.9565
.85	.8870	1.0274	-.7389	-30.5838
.90	.9363	.9011	-6.1344	-267.8938
.95	.9827	-.2388	-57.7441	-2673.4115
1.00	.7646	-11.9381	-616.7769	-30037.4470

(i) $Re_{d,w} = 98$ (suction) $\delta^*/h = 0.0206$
$f_2'(0) = 1.0430000$ $f_2'(1) = -11.3912$
$A_2 = 53.313962$

f_2	f_2'	f_2''	f_2'''	η_2
0.0000	1.0430	0.0000	0.0094	0.00
.0522	1.0430	.0005	.0094	.05
.1043	1.0430	.0009	.0094	.10
.1565	1.0431	.0014	.0094	.15
.2086	1.0432	.0019	.0094	.20
.2608	1.0433	.0023	.0094	.25
.3129	1.0434	.0028	.0094	.30
.3651	1.0436	.0033	.0094	.38
.4173	1.0437	.0037	.0094	.40
.4695	1.0439	.0042	.0095	.45
.5217	1.0442	.0047	.0096	.50
.5739	1.0444	.0052	.0102	.55
.6261	1.0447	.0058	.0128	.60
.6784	1.0450	.0066	.0246	.65
.7306	1.0454	.0090	.0881	.70
.7829	1.0460	.0202	.4741	.75
.8353	1.0483	.0898	3.1449	.80
.8879	1.0614	.5985	24.1516	.85
.9427	1.1620	4.8664	211.9331	.90
1.0155	2.0650	45.7547	2121.1319	.95
1.2669	11.3912	484.4472	24386.7180	1.00

(j) $Re_{d,w} = 98$ (suction) $\delta^*/h = 0.0206$
$f_2(0) = 1.0430000$ $f_2'(1) = 0.6929$
$A_2 = 53.313961$

η_2	f_2	f_2'	f_2''	f_2'''
0.00	0.0000	1.0430	0.0000	0.0094
.05	.0522	1.0430	.0005	.0094
.10	.1043	1.0430	.0009	.0094
.15	.1565	1.0431	.0014	.0094
.20	.2086	1.0432	.0019	.0094
.25	.2608	1.0433	.0023	.0094
.30	.3129	1.0434	.0028	.0094
.35	.3651	1.0436	.0033	.0094
.40	.4173	1.0437	.0037	.0094
.45	.4695	1.0439	.0042	.0094
.50	.5217	1.0442	.0047	.0094
.55	.5739	1.0444	.0052	.0094
.60	.6261	1.0447	.0056	.0093
.65	.6784	1.0450	.0061	.0089
.70	.7306	1.0453	.0065	.0078
.75	.7829	1.0456	.0066	-.0068
.80	.8352	1.0459	.0047	-.0096
.85	.8875	1.0459	-.0120	-.3374
.90	.9397	1.0429	-.1569	-.7011
.95	.9914	1.0125	-1.5574	-72.5759
1.00	1.0370	.6929	-16.9776	-832.8548

TABLE II. - NUMERICAL SOLUTIONS FOR SEMIPOROUS DUCT

(a) $Re_{d,w} = -20$ (ejection) $A_1 = -65.3486$
$f_1''(0) = 13.0036$ $(\delta^*/h)_p = 0.2751$

η_1	f_1	f_1'	f_1''	f_1'''
0.00	0.0000	0.0000	13.0036	- 65.3486
.05	.0149	.5693	9.7984	- 61.7868
.10	.0544	.9861	6.9042	- 53.4465
.15	.1112	1.2677	4.4854	- 43.1814
.20	.1793	1.4423	2.5841	- 33.0112
.25	.2540	1.5341	1.1616	- 24.1798
.30	.3317	1.5651	.1343	- 17.2501
.35	.4098	1.5525	- .5957	- 12.2604
.40	.4865	1.5089	- 1.1191	- 8.9221
.45	.5603	1.4428	- 1.5082	- 6.8118
.50	.6305	1.3595	- 1.8137	- 5.5142
.55	.6961	1.2683	- 2.0675	- 4.6978
.60	.7565	1.1533	- 2.2876	- 4.1344
.65	.8112	1.0339	- 2.4828	- 3.6851
.70	.8597	.9054	- 2.6566	- 3.2737
.75	.9016	.7686	- 2.8098	- 2.8644
.80	.9365	.6247	- 2.9417	- 2.4463
.85	.9640	.4747	- 3.0501	- 2.0345
.90	.9839	.3198	- 3.1304	- 1.7040
.95	.9959	.1611	- 3.1673	- 1.7418
1.00	1.0000	.0000	- 3.1067	- 3.2192

(b) $Re_{d,w} = -10$ (ejection) $A_1 = 38.1025$
$f_1''(0) = 10.0368$ $(\delta^*/h)_p = 0.2419$

f_1	f_1'	f_1''	f_1'''	η_1
0.0000	0.0000	10.0368	- 38.1025	0.00
.0118	.4545	8.1507	- 36.9953	.05
.0439	.8168	6.3649	- 34.2861	.10
.0920	1.0937	4.7439	- 30.5053	.15
.1520	1.2945	3.3208	- 26.3940	.20
.2204	1.4292	2.1039	- 22.3116	.25
.2940	1.5081	1.0843	- 18.5451	.30
.3704	1.5406	.2413	- 15.2617	.35
.4474	1.5348	- .4511	- 12.5284	.40
.5234	1.4975	- 1.0205	- 10.3382	.45
.5967	1.4344	- 1.4926	- 8.6216	.50
.6664	1.3495	- 1.8892	- 7.2998	.55
.7314	1.2464	- 2.2275	- 6.2752	.60
.7908	1.1276	- 2.5202	- 5.4592	.65
.8439	.9950	- 2.7756	- 4.7776	.70
.8901	.8505	- 2.9992	- 4.1727	.75
.9288	.6956	- 3.1935	- 3.6089	.80
.9595	.5316	- 3.3596	- 3.0403	.85
.9818	.3601	- 3.4974	- 2.4675	.90
.9954	.1824	- 3.6060	- 1.8748	.95
1.0000	.0000	- 3.6844	- 1.2582	1.00

(c) $Re_{d,w} = -8$ (ejection) $A_1 = -32.6554$
$f_1''(0) = 9.3296$ $(\delta^*/h)_p = 0.2518$

η_1	f_1	f_1'	f_1''	f_1'''
0.00	0.0000	0.0000	9.3296	- 32.6554
.05	.0110	.4258	7.7101	- 31.8822
.10	.0413	.7722	6.1611	- 29.9186
.15	.0870	1.0439	4.7303	- 27.2279
.20	.1445	1.2477	3.4442	- 24.1843
.25	.2107	1.3909	2.3129	- 21.0768
.30	.2827	1.4815	1.3341	- 18.1144
.35	.3581	1.5267	.4968	- 15.4321
.40	.4348	1.5333	- .2150	- 13.1006
.45	.5109	1.5070	- .8195	- 11.1362
.50	.5850	1.4528	- 1.3346	- 9.5244
.55	.6558	1.3747	- 1.7770	- 8.2141
.60	.7221	1.2761	- 2.1601	- 7.1492
.65	.7831	1.1595	- 2.4949	- 6.2695
.70	.8378	1.0273	- 2.7892	- 5.5185
.75	.8856	.8812	- 3.0481	- 4.8485
.80	.9257	.7230	- 3.2748	- 4.2213
.85	.9577	.5542	- 3.4705	- 3.6084
.90	.9810	.3764	- 3.6355	- 2.9901
.95	.9952	.1912	- 3.7698	- 2.3534
1.00	1.0000	.0001	- 3.8704	- 1.6912

(d) $Re_{d,w} = -4$ (ejection) $A_1 = -21.9473$
$f_1''(0) = 7.7620$ $(\delta^*/h)_p = 0.2049$

f_1	f_1'	f_1''	f_1'''	η_1
0.0000	0.0000	7.7620	- 21.9473	0.00
.0092	.3607	6.6693	- 21.6735	.05
.0352	.6674	5.6021	- 20.9539	.10
.0751	.9217	4.5791	- 19.9251	.15
.1265	1.1262	3.6128	- 18.7020	.20
.1870	1.2840	2.7105	- 17.3794	.25
.2542	1.3984	1.8753	- 16.0320	.30
.3261	1.4727	1.1068	- 14.7161	.35
.4008	1.5101	.4025	- 13.4705	.40
.4766	1.5139	- .2418	- 12.3185	.45
.5517	1.4869	- .8311	- 11.2699	.50
.6248	1.4316	- 1.3705	- 10.3237	.55
.6945	1.3506	- 1.8650	- 9.4704	.60
.7595	1.2458	- 2.3188	- 8.6948	.68
.8187	1.1193	- 2.7355	- 7.9781	.70
.8711	.9729	- 3.1173	- 7.3002	.75
.9157	.8081	- 3.4658	- 6.6411	.80
.9516	.6268	- 3.7814	- 5.9822	.85
.9781	.4306	- 4.0637	- 5.3070	.90
.9944	.2810	- 4.3116	- 4.6016	.95
1.0000	.0000	- 4.5232	- 3.8545	1.00

TABLE II. - Concluded. NUMERICAL SOLUTIONS FOR SEMIPOROUS DUCT

(e) $Re_{d,w} = 4$ (suction) $A_1 = -3.7516$
$f_1''(0) = 4.1699$ $(\delta^*/h)_p = 0.1219$

η_1	f_1	f_1'	f_1''	f_1'''
0.00	0.0000	0.0000	4.1699	-3.7516
.05	.0051	.2038	3.9809	-3.8360
.10	.0202	.3980	3.7837	-4.0791
.15	.0448	.5819	3.5706	-4.4667
.20	.0782	.7546	3.3348	-4.9861
.25	.1200	.9149	3.0700	-5.6259
.30	.1695	1.0610	2.7703	-6.3769
.35	.2259	1.1912	2.4305	-7.2321
.40	.2883	1.3033	2.0455	-8.1877
.45	.3558	1.3950	1.6101	-9.2434
.50	.4274	1.4634	1.1194	-10.4045
.55	.5018	1.5059	.5677	-11.6829
.60	.5775	1.5191	-.0512	-13.1004
.65	.6531	1.4995	-.7452	-14.6926
.70	.7268	1.4431	-1.5243	-16.5140
.75	.7967	1.3454	-2.4018	-18.6469
.80	.8606	1.2010	-3.3961	-21.2185
.85	.9160	1.0035	-4.5331	-24.3880
.90	.9599	.7447	-5.8493	-28.4300
.95	.9892	.4147	-7.3966	-33.7078
1.00	1.0000	.0000	-9.2493	-40.7487

(f) $Re_{d,w} = 10$ (suction) $A_1 = 4.8506$
$f_1''(0) = 1.5982$ $(\delta^*/h)_p = 0.0703$

f_1	f_1'	f_1''	f_1'''	η_1
0.0000	0.0000	1.5982	4.8506	0.00
.0021	.0860	1.8401	4.8153	.05
.0088	.1840	2.0783	4.6950	.10
.0207	.2937	2.3078	4.4657	.15
.0383	.4145	2.5286	4.0999	.20
.0623	.5455	2.7150	3.5661	.25
.0931	.6855	2.8758	2.8279	.30
.1310	.8324	2.9937	1.8424	.35
.1764	.9839	3.0551	.5582	.40
.2294	1.1367	3.0435	-1.0891	.45
.2900	1.2867	2.9388	-3.1831	.50
.3579	1.4286	2.7159	-5.8381	.55
.4326	1.5558	2.3429	-9.2185	.60
.5131	1.6597	1.7779	-13.5732	.65
.5980	1.7294	.9630	-19.2999	.70
.6852	1.7505	-.1856	-27.0627	.75
.7719	1.7032	-1.7957	-38.0205	.80
.8540	1.5598	-4.0743	-54.2736	.85
.9256	1.2789	-7.3738	-79.7591	.90
.9785	.7952	-12.3841	-122.0652	.95
1.0000	.0000	-20.0963	-196.1123	1.00

(g) $Re_{d,w} = 13$ (suction) $A_1 = 9.1350$
$f_1''(0) = 0.0855$ $(\delta^*/h)_p = 0.0551$

η_1	f_1	f_1'	f_1''	f_1'''
0.00	0.0000	0.0000	0.0855	9.1350
.05	.0003	.0157	.5423	9.1339
.10	.0019	.0542	.9987	9.1221
.15	.0061	.1155	1.4539	9.0768
.20	.0139	.1996	1.9053	8.9612
.25	.0264	.3059	2.3480	8.7250
.30	.0448	.4341	2.7747	8.3028
.35	.0702	.5829	3.1739	7.6131
.40	.1034	.7508	3.5298	6.5549
.45	.1455	.9349	3.8212	5.0028
.50	.1971	1.1313	4.0193	2.7972
.55	.2588	1.3346	4.0865	-.2728
.60	.3306	1.5370	3.9728	-4.5007
.65	.4123	1.7278	3.6101	-10.3226
.70	.5029	1.8923	2.9088	-18.4346
.75	.6007	2.0100	1.7094	-3 .0354
.80	.7027	2.0514	-.1940	-47.3467
.85	.8039	1.9725	-3.1897	-74.7803
.90	.8968	1.7028	-7.9861	-121.6604
.95	.9690	1.1210	-16.0022	-208.7866
1.00	1.0000	.0000	-30.2825	-384.5379

TABLE III. - NUMERICAL SOLUTIONS FOR POROUS TUBE

(a) $Re_{t,w} = -10$ (ejection) $\delta^*/h = 0.2588$
$f_t''(1) = -1.2052$ $\eta_t f_t'''(0) = 0.0093$
$A_t = -7.4782$

η_t	f_t	f_t'	f_t''	f_t'''
1.00	0.5000	0.0000	-1.2052	-0.2441
.95	.4985	.0599	-1.1909	-.3284
.90	.4940	.1190	-1.1724	-.4104
.85	.4866	.1771	-1.1499	-.4898
.80	.4763	.2339	-1.1234	-.5664
.75	.4632	.2894	-1.0933	-.6401
.70	.4474	.3432	-1.0595	-.7106
.65	.4290	.3953	-1.0223	-.7778
.60	.4079	.4454	-.9818	-.8416
.55	.3845	.4934	-.9382	-.9018
.50	.3586	.5391	-.8916	-.9582
.45	.3306	.5825	-.8424	-1.0109
.40	.3004	.6233	-.7906	-1.0596
.35	.2683	.6615	-.7365	-1.1044
.30	.2343	.6970	-.6803	-1.1452
.25	.1986	.7295	-.6221	-1.1819
.20	.1614	.7591	-.5621	-1.2145
.15	.1228	.7857	-.5007	-1.2428
.10	.0829	.8092	-.4379	-1.2652
.05	.0419	.8295	-.3744	-1.2668
.00	.0000	.8467	-.3158	-1.3389

(b) $Re_{t,w} = -4$ (ejection) $\delta^*/R = 0.2838$
$f_t''(1) = -1.1531$ $\eta_t f_t'''(0) = -0.0002$
$A_t = -3.7023$

f_t	f_t'	f_t''	f_t'''	η_t
0.5000	0.0000	-1.1531	-0.2430	1.00
.4986	.0573	-1.1398	-.2910	.95
.4943	.1139	-1.1240	-.3378	.90
.4872	.1697	-1.1060	-.3833	.85
.4773	.2245	-1.0857	-.4275	.80
.4648	.2782	-1.0633	-.4704	.75
.4495	.3308	-1.0387	-.5118	.70
.4317	.3821	-1.0121	-.5517	.65
.4113	.4320	-.9836	-.5901	.60
.3885	.4804	-.9531	-.6269	.55
.3633	.5273	-.9209	-.6622	.50
.3358	.5725	-.8869	-.6958	.45
.3061	.6159	-.8514	-.7278	.40
.2743	.6576	-.8142	-.7582	.35
.2404	.6973	-.7756	-.7868	.30
.2046	.7351	-.7355	-.8138	.25
.1669	.7709	-.6942	-.8391	.20
.1275	.8045	-.6517	-.8627	.15
.0865	.8360	-.6080	-.8847	.10
.0439	.8653	-.5632	-.9054	.05
.0000	.8923	-.5174	-.9234	.00

(c) $Re_{t,w} = -2$ (ejection) $\delta^*/R = 0.3014$
$f_t''(1) = -1.1054$ $\eta_t f_t'''(0) = 0.0001$
$A_t = -2.3980$

η_t	f_t	f_t'	f_t''	f_t'''
1.00	0.5000	0.0000	-1.1054	-0.1871
.95	.4986	.0550	-1.0954	-.3149
.90	.4945	.1095	-1.0840	-.2422
.85	.4877	.1634	-1.0712	-.2690
.80	.4782	.2166	-1.0571	-.2952
.75	.4660	.2691	-1.0417	-.3209
.70	.4513	.3208	-1.0250	-.3459
.65	.4340	.3716	-1.0071	-.3703
.60	.4141	.4214	-.9880	-.3942
.55	.3918	.4703	-.9677	-.4174
.50	.3671	.5182	-.9462	-.4399
.45	.3400	.5649	-.9237	-.4618
.40	.3106	.6105	-.9001	-.4830
.35	.2790	.6549	-.8754	-.5035
.30	.2452	.6981	-.8497	-.5233
.25	.2092	.7399	-.8231	-.5425
.20	.1712	.7804	-.7955	-.5609
.15	.1312	.8194	-.7670	-.5787
.10	.0893	.8570	-.7376	-.5958
.05	.0455	.8932	-.7074	-.6124
.00	.0000	.9278	-.6764	-.6276

(d) $Re_{t,w} = 1$ (suction) $\delta^*/R = 0.3627$
$f_t''(1) = -0.8823$ $\eta_t f_t'''(0) = 0.0000$
$A_t = -0.1909547$

f_t	f_t'	f_t''	f_t'''	η_t
0.5000	0.0000	-0.8823	0.2502	1.00
.4989	.0444	-.8953	.2692	.95
.4955	.0895	-.9092	.2885	.90
.4899	.1354	-.9241	.3084	.85
.4820	.1820	-.9401	.3286	.80
.4717	.2294	-.9570	.3493	.75
.4590	.2777	-.9750	.3705	.70
.4439	.3269	-.9941	.3922	.65
.4263	.3771	-1.0142	.4144	.60
.4062	.4284	-1.0355	.4372	.55
.3835	.4807	-1.0580	.4605	.50
.3581	.5342	-1.0816	.4844	.45
.3300	.5889	-1.1064	.5088	.40
.2992	.6448	-1.1325	.5339	.35
.2655	.7021	-1.1598	.5596	.30
.2290	.7608	-1.1885	.5860	.25
.1894	.8210	-1.2184	.6131	.20
.1468	.8827	-1.2498	.6409	.15
.1011	.9460	-1.2825	.6694	.10
.0522	1.0110	-1.3167	.6987	.05
.0000	1.0777	-1.3524	.7287	.00

TABLE III. - Concluded. NUMERICAL SOLUTIONS FOR POROUS TUBE

(e) $Re_{t,w} = 2$ (suction) $\delta^*/R = 0.4257$
$f_t''(1) = -0.5633$ $\eta_t f_t'''(0) = 0.0000$
$A_t = 0.9807$

η_t	f_t	f_t'	f_t''	f_t'''
1.00	0.5000	0.0000	-0.5633	0.9807
.95	.4993	.0294	-.6136	1.0315
.90	.4970	.0614	-.6665	1.0857
.85	.4931	.0961	-.7223	1.1438
.80	.4874	.1337	-.7810	1.2059
.75	.4797	.1743	-.8429	1.2724
.70	.4699	.2180	-.9083	1.3434
.65	.4578	.2652	-.9774	1.4194
.60	.4433	.3158	-1.0503	1.5006
.55	.4262	.3703	-1.1275	1.5874
.50	.4062	.4287	-1.2092	1.6801
.45	.3832	.4913	-1.2956	1.7792
.40	.3570	.5583	-1.3872	1.8851
.35	.3273	.6301	-1.4842	1.9982
.30	.2939	.7068	-1.5871	2.1189
.25	.2565	.7889	-1.6963	2.2479
.20	.2149	.8766	-1.8121	2.3855
.15	.1688	.9702	-1.9350	2.5324
.10	.1178	1.0702	-2.0655	2.6892
.05	.0617	1.1769	-2.2041	2.8565
.00	.0000	1.2907	-2.3513	3.0348

(f) $Re_{t,w} = 2$ (suction) $\delta^*/R = 0.4210$
$f_t''(1) = 1.1844$ $\eta_t f_t'''(0) = -0.0002$
$A_t = 4.5934$

f_t	f_t'	f_t''	f_t'''	η_t
0.5000	0.0000	1.1844	4.5934	1.00
.5014	.0534	.9488	4.8320	.95
.5051	.0947	.7008	5.0919	.90
.5106	.1232	.4393	5.3793	.85
.5172	.1383	.1623	5.7009	.80
.5242	.1392	-.1316	6.0644	.75
.5309	.1249	-.4450	6.4782	.70
.5364	.0943	-.7804	6.9519	.65
.5400	.0464	-1.1413	7.4962	.60
.5408	.0203	-1.5314	8.1231	.55
.5377	.1073	-1.9552	8.8461	.50
.5297	.2165	-2.4179	9.6804	.45
.5156	.3499	-2.9254	10.6431	.40
.4942	.5099	-3.4847	11.7531	.35
.4641	.6993	-4.1035	13.0320	.30
.4238	.9214	-4.7911	14.5040	.25
.3714	1.1797	-5.5576	16.1962	.20
.3051	1.4787	-6.4149	18.1391	.15
.2228	1.8230	-7.3763	20.3672	.10
.1220	2.2183	-8.4570	22.9187	.05
.0000	2.6709	-9.6742	25.8391	.00

(g)[1] $Re_{t,w} = 10$ (suction) $A_t = 3.3058$
$f_t''(1) = -2.2940$ $\eta_t f_t'''(0) = 0.0000$

η_t	f_t	f_t'	f_t''	f_t'''
1.00	0.5000	0.0000	-2.2940	-5.8703
.95	.4973	.1077	-2.0208	-5.0924
.90	.4894	.2026	-1.7818	-4.4933
.85	.4772	.2863	-1.5691	-4.0378
.80	.4610	.3599	-1.3761	-3.6961
.75	.4413	.4242	-1.1980	-3.4435
.70	.4187	.4799	-1.0307	-3.2594
.65	.3935	.5274	-.8712	-3.1266
.60	.3661	.5671	-.7174	-3.0313
.55	.3369	.5992	-.5676	-2.9620
.50	.3063	.6239	-.4209	-2.9096
.45	.2746	.6413	-.2765	-2.8664
.40	.2423	.6516	-.1342	-2.8264
.35	.2096	.6548	.0061	-2.7847
.30	.1769	.6510	.1442	-2.7374
.25	.1446	.6404	.2797	-2.6814
.20	.1130	.6231	.4121	-2.6143
.15	.0824	.5992	.5409	-2.5341
.10	.0532	.5691	.6653	-2.4395
.05	.0256	.5328	.7846	-2.3294
.00	.0000	.4907	.8980	-2.2032

(h)[1] $Re_{t,w} = 10$ (suction) $A_t = 2.0666$
$f_t''(1) = -4.0122$ $\eta_t f_t'''(0) = -0.0001$

f_t	f_t'	f_t''	f_t'''	η_t
0.5000	0.0000	-4.0122	-13.9822	1.00
.4953	.1839	-3.3608	-12.1639	.95
.4821	.3374	-2.7882	-10.8062	.90
.4620	.4637	-2.2745	-9.7851	.85
.4361	.5656	-1.8057	-9.0025	.80
.4058	.6449	-1.3716	-8.3820	.75
.3720	.7032	-.9658	-7.8649	.70
.3358	.7419	-.5841	-7.4068	.65
.2981	.7620	-.2246	-6.9747	.60
.2599	.7647	.1134	-6.5447	.55
.2219	.7510	.4296	-6.0998	.50
.1850	.7221	.7229	-5.6289	.45
.1500	.6791	.9919	-5.1252	.40
.1173	.6234	1.2348	-4.5854	.35
.0878	.5561	1.4499	-4.0091	.30
.0619	.4789	1.6352	-3.3979	.25
.0401	.3931	1.7891	-2.7554	.20
.0227	.3005	1.9103	-2.0864	.15
.0101	.2027	1.9974	-1.3968	.10
.0025	.1013	2.0497	-.6932	.05
.0000	.0017	2.0667	-.1776	.00

[1]Calculations for δ^*/R were not made because $f'_{t,max}$ was not at center of channel.

TABLE IV. - NUMERICAL SOLUTIONS FOR POROUS WEDGE

(a) $f_{b,w} = -2.0$, $f_b''(0) = 0.4758$, $Eu = 1.0$, $\frac{\delta^*\sqrt{Re_x}}{x} = 1.3618$

η_b	f_b	f_b'	f_b''	f_b'''
0.00	-2.0000	0.0000	0.4758	-0.0484
.20	-1.9906	.0941	.4642	-.0670
.40	-1.9626	.1855	.4491	-.0842
.60	-1.9166	.2735	.4307	-.0998
.80	-1.8534	.3575	.4093	-.1136
1.00	-1.7739	.4370	.3853	-.1254
1.20	-1.6789	.5115	.3598	-.1352
1.40	-1.5696	.5806	.3314	-.1427
1.60	-1.4471	.6440	.3023	-.1478
1.80	-1.3124	.7015	.2725	-.1503
2.00	-1.1669	.7530	.2424	-.1502
2.20	-1.0116	.7985	.2126	-.1474
2.40	-.8479	.8381	.1836	-.1419
2.60	-.6768	.8720	.1560	-.1340
2.80	-.4994	.9006	.1301	-.1239
3.00	-.3169	.9242	.1065	-.1121
3.20	-.1301	.9434	.0854	-.0990
3.40	.0602	.9585	.0670	-.0852
3.60	.2531	.9703	.0513	-.0714
3.80	.4481	.9793	.0384	-.0583
4.00	.6447	.9858	.0279	-.0461
4.20	.8423	.9906	.0198	-.0354
4.40	1.0408	.9939	.0137	-.0264
4.60	1.2398	.9962	.0091	-.0190
4.80	1.4392	.9976	.0059	-.0133
5.00	1.6389	.9986	.0037	-.0089
5.20	1.8386	.9992	.0023	-.0058
5.40	2.0385	.9995	.0014	-.0037
5.60	2.2384	.9998	.0008	-.0022
5.80	2.4384	.9999	.0004	-.0013
6.00	2.6384	.9999	.0002	-.0007
6.20	2.8384	1.0000	.0001	-.0004
6.40	3.0384	1.0000	.0001	-.0002
6.60	3.2384	1.0000	.0000	-.0001
6.80	3.4384	1.0000	.0000	-.0001
7.00	3.6384	1.0000	.0000	.0000
7.20	3.8384	1.0000	.0000	.0000
7.40	4.0384	1.0000	.0000	.0000

(b) $f_{b,w} = -3.0$, $f_b''(0) = 0.3295$, $Eu = 1.0$, $\frac{\delta^*\sqrt{Re_x}}{x} = 1.8581$

f_b	f_b'	f_b''	f_b'''	η_b
-3.0000	0.0000	0.3295	-0.0116	0.00
-2.9934	.0656	.3264	-.0185	.20
-2.9738	.1305	.3220	-.0253	.40
-2.9413	.1943	.3163	-.0318	.60
-2.8962	.2569	.3093	-.0381	.80
-2.8386	.3180	.3011	-.0441	1.00
-2.7691	.3773	.2917	-.0498	1.20
-2.6878	.4346	.2812	-.0552	1.40
-2.5954	.4897	.2697	-.0602	1.60
-2.4921	.5424	.2572	-.0649	1.80
-2.3786	.5925	.2438	-.0691	2.00
-2.2553	.6399	.2296	-.0728	2.20
-2.1228	.6843	.2147	-.0760	2.40
-1.9818	.7257	.1992	-.0786	2.60
-1.8327	.7640	.1833	-.0805	2.80
-1.6764	.7990	.1670	-.0816	3.00
-1.5134	.8308	.1507	-.0818	3.20
-1.3443	.8593	.1343	-.0811	3.40
-1.1699	.8845	.1183	-.0792	3.60
-.9907	.9066	.1027	-.0763	3.80
-.8074	.9256	.0879	-.0722	4.00
-.6207	.9417	.0738	-.0673	4.20
-.4309	.9552	.0609	-.0613	4.40
-.2388	.9662	.0493	-.0547	4.60
-.446	.9750	.0391	-.0476	4.80
.1511	.9819	.0303	-.0404	5.00
.3481	.9872	.0229	-.0334	5.20
.5459	.9912	.0169	-.0268	5.40
.7445	.9941	.0121	-.0209	5.60
.9435	.9961	.0085	-.0158	5.80
1.1429	.9975	.0058	-.0116	6.00
1.3425	.9985	.0038	-.0082	6.20
1.5422	.9991	.0024	-.0056	6.40
1.7421	.9995	.0015	-.0037	6.60
1.9420	.9997	.0009	-.0024	6.80
2.1419	.9998	.0005	-.0015	7.00
2.3419	.9999	.0003	-.0009	7.20
2.5419	1.0000	.0002	-.0005	7.40
2.7419	1.0000	.0001	-.0003	7.60
2.9419	1.0000	.0000	-.0001	7.80
3.1419	1.0000	.0000	-.0001	8.00
3.3419	1.0000	.0000	.0000	8.20
3.5419	1.0000	.0000	.0000	8.40

TABLE IV. - Concluded. NUMERICAL SOLUTIONS FOR POROUS WEDGE

(c)

$f_{b,w} = -2.0$ $\quad$ $Eu = 0.5$

$f_b''(0) = 0.32446$ $\quad$ $\frac{\delta^* \sqrt{Re_x}}{x} = 1.8464$

η_b	f_b	f_b'	f_b''	f_b'''
0.00	-2.0000	0.0000	0.3245	- 0.0133
.20	-1.9935	.0646	.3214	- .0174
.40	-1.9742	.1285	.3175	- .0216
.60	-1.9422	.1915	.3127	- .0261
.80	-1.8977	.2535	.3070	- .0309
1.00	-1.8409	.3143	.3003	- .0359
1.20	-1.7720	.3736	.2926	- .0413
1.40	-1.6915	.4313	.2838	- .0470
1.60	-1.5997	.4870	.2738	- .0529
1.80	-1.4968	.5407	.2627	- .0590
2.00	-1.3835	.5920	.2502	- .0651
2.20	-1.2602	.6407	.2366	- .0711
2.40	-1.1274	.6866	.2218	- .0767
2.60	- .9858	.7294	.2060	- .0817
2.80	- .8359	.7689	.1892	- .0857
3.00	- .6784	.8050	.1718	- .0886
3.20	- .5141	.8376	.1539	- .0899
3.40	- .3436	.8666	.1359	- .0895
3.60	- .1677	.8920	.1182	- .0873
3.80	.0129	.9139	.1011	- .0833
4.00	.1976	.9325	.0850	- .0778
4.20	.3857	.9480	.0701	- .0709
4.40	.5767	.9607	.0567	- .0631
4.60	.7698	.9708	.0449	- .0547
4.80	.9648	.9787	.0348	- .0462
5.00	1.1612	.9848	.0264	- .0380
5.20	1.3587	.9894	.0196	- .0305
5.40	1.5569	.9928	.0142	- .0237
5.60	1.7557	.9952	.0100	- .0180
5.80	1.9549	.9968	.0069	- .0133
6.00	2.1544	.9980	.0046	- .0095
6.20	2.3541	.9987	.0030	- .0066
6.40	2.5539	.9992	.0019	- .0045
6.60	2.7538	.9995	.0012	- .0029
6.80	2.9537	.9997	.0007	- .0019
7.00	3.1537	.9999	.0004	- .0012
7.20	3.3537	.9999	.0002	- .0007
7.40	3.5536	1.0000	.0001	- .0004
7.60	3.7536	1.0000	.0001	- .0002
7.80	3.9536	1.0000	.0000	- .0001
8.00	4.1536	1.0000	.0000	- .0001
8.20	4.3536	1.0000	.0000	.0000
8.40	4.5536	1.0000	.0000	.0000
8.60	4.7536	1.0000	.0000	.0000
8.80	4.9536	1.0000	.0000	.0000

4518

4518

TABLE V. - SUMMARY OF DIMENSIONLESS PARAMETERS FOR THE DIFFERENT GEOMETRIES

(a) Fully porous channel

	$Re_{d,w}$	A_2	$f_2'(0)$	$(2\delta^*/h)_2$	Φ_2	$\tau_{2,x}$	T_2	Additional information: Reference	Additional information: Page or table*
Ejection	-20	-27.028	1.5380	0.17489	-3.4978	-2.1501	1.2000		I(a)
	-10	-14.870	1.5252	.17217	-1.7217	-1.1560	1.2366		I(b)
	-4	-7.698	1.5199	.17102	-.6841	-.5926	1.2909	4	18
	-2	-5.3303	1.5066	.16814	-.3363	-.4001	1.3049		I(c)
	0	-3	1.5000	.16667	0	-.2222	1.3334	4	18
Suction	2	-0.7046	1.4923	0.16494	0.3299	-0.0514	1.3689		I(d)
	10	7.9139	1.4473	.15453	1.5453	.5223	1.6236		I(e)
	20	16.478	1.3549	.13097	2.6194	.8344	2.3189		I(f)
	40	26.055	1.1551	.06714	2.6856	.4067	3.6513		I(g)
	98	53.314	1.0430	.0206	2.019	.0868			I(h), (i), or (j)

(b) Semiporous channel

		$Re_{d,w}$	A_1	$f_1''(0)$	$(\delta^*/h)_1$	Φ_1	$\tau_{1,x}$	T_1	Additional information: Reference	Additional information: Page or table*
Ejection	Porous	-20	-65.350	13.004	0.2731	-5.462	-3.1132	1.1310		II(a)
	solid	0	-65.350	13.004	.0882	0	-.3247	1.4652		II(a)
	porous	-10	-38.103	10.037	.2419	-2.419	-1.4454	1.1555		II(b)
	solid	0	-38.103	10.037	.1099	0	-.2983	1.4301		II(b)
	porous	-8	-32.655	9.3296	.2318	-1.854	-1.1426	1.1688		II(c)
	solid	0	-32.655	9.3296	.1167	0	-.2899	1.4192		II(c)
	porous	-4	-21.947	7.7620	.2049	-.8196	-.6077	1.2225		II(d)
	solid	0	-21.947	7.7620	.1356	0	-.2661	1.3883		II(d)
	porous	-3	-19.36	7.336	.1965	-.5895	-.4948	1.2439	4	18
	solid	0	-19.36	7.336	.1416	0	-.2570	1.3752		
	porous	-2	-16.82	6.900	.1870	-.3740	-.3905	1.2685		
	solid	0	-16.82	6.900	.1490	0	-.2479	1.3653		
	porous	-1	-14.37	6.454	.1772	-.1772	-.3003	1.2996		
	solid	0	-14.37	6.454	.1573	0	-.2366	1.3513		
	porous	0	-12	6	.1667	0	-.2222	1.3336		
	solid	0	-12	6	.1667	0	-.2222	1.3336		
Suction	Porous	1	-9.742	5.542	0.1557	0.1557	-0.1575	1.3706	4	18
	solid	0	-9.742	5.542	.1774	0	-.2045	1.3113	4	18
	porous	4	-3.7516	4.1699	.1219	.4876	-.0367	1.4843		II(e)
	solid	0	-3.7516	4.1699	.2199	0	-.1194	1.2072		II(e)
	porous	10	4.8506	1.5982	.0703	.703	.0137	1.6135		II(f)
	solid	0	4.8506	1.5982	.3586	0	.3562	.6546		II(f)
	porous	13	9.1350	.0855	.0551	.716	.0136	1.6258		II(g)
	solid	0	9.1350	.0855	.4577	0	.9323	.3813		II(g)

(c) Porous tube

	$Re_{t,w}$	A_t	$f_t''(1)$	$(\delta^*/R)_t$	Φ_t	$\tau_{t,x}$	T_t	Additional information: Reference	Additional information: Page or table*
Ejection	-10	-7.4751	-1.2052	0.2589	-2.5894	-1.1841	1.4744		III(a)
	-4	-3.7023	-1.1531	.2838	-1.1352	-.6683	1.4669		III(b)
	-2	-2.3980	-1.1054	.3014	-.6028	-.4695	1.4364		III(c)
	0	-1	-1	.3333	0	-.2222	1.3333	5	720, 721
Suction	1	-0.1910	-0.8823	0.3627	-0.3627	-0.0466	1.1878		III(d)
	2	.9807	-.5633	.4257	.8514	.2754	.7432		III(e)
	2	4.5934	1.1844	.4210	.8420	.6097	.7468		III(f)
	10	3.3058	-2.2940						III(g)
	10	2.0666	-4.0122						III(h)

*Roman numerals indicate tables in present report.

TABLE V. - Continued. SUMMARY OF DIMENSIONLESS PARAMETERS FOR THE DIFFERENT GEOMETRIES

(d) Porous wedge

	$f_{b,w}$	Eu	$f_b''(0)$	$\frac{\delta^*\sqrt{Re_x}}{x} = B$	Φ_b	$\tau_{b,x}$	T_b	Additional information	
								Reference	Page or table
Ejection	-4.3346	1.0	0.2300	2.5734	-11.1547	-6.6224	1.1838	23	63
	-3.1905	1.0	.3106	1.9585	-6.2486	-3.8357	1.2186	23	63
	-3	1.0	.32945	1.8581	-5.5743	-3.4525	1.2243	This report	IV(b)
	-2	.5	.32446	1.8464	-2.7696	-1.70460	1.1982		IV(c)
	-2	1.0	.47581	1.3616	-2.7232	-1.8540	1.2957		IV(a)
	-1.4618	.11111	.15116	2.8911	-2.3479	-.92871	.8740	22	12
	-1.23849	0	0	19.29038	-11.9455	0	0	21	
	-1.2	0	.0033575	7.85212	-4.7113	0	.052727	21	
	-1.198	1.0	.6864	1.0180	-1.2196	-1.0383	1.3975	23	63
	-1.15	0	.00965	6.25417	-3.5961	0	.12071	21	
	-1.10	0	.01728	5.40261	-2.9714	0	.18671	21	
	-1.05	0	.0259575	4.82483	-2.5330	0	.25048	21	
	-1.0	-.0072	0	6.398	-3.1780	.2947	0	20	39
		0	.0355175	4.39079	-2.1954	0	.31190	13,21,23	18,*,46
		.05	.1410	2.796	-1.4679	-.3909	.7885	20	41
		.15	.2703	2.008	-1.1546	-.6048	1.0885	20	42
		.5	.5345	1.260	-.945	-.7938	1.3469	13	19
		1.0	.7585	.945	-.945	-.8930	1.4298	13	20
	-.95	0	.04586	4.04534	-1.9215	0	.37104	21	
	-.9382	.11111	.2391	2.1452	-1.1181	-.51132	1.0258	22	12
	-.90	0	.058895	3.76021	-1.6921	0	.42787	21	
	-.85	0	.0685675	3.51861	-1.4954	0	.48252	21	
	-.80	0	.080820	3.30988	-1.3240	0	.53501	21	
	-.75	0	.0936125	3.12895	-1.1726	0	.58544	21,23	*,46
	-.70	0	.1089050	2.96469	-1.0376	0	.63388	21	
	-.65	0	.1206675	2.81935	-.91629	0	.68041		
	-.60	0	.1348700	2.68814	-.80644	0	.72510		
	-.55	0	.149485	2.56880	-.70642	0	.76799		
	-.5	-.0418	0	4.272	-1.0234	.7628	0	20	28
		0	.16449	2.4599	-.61498	0	.80926	13,20,21,23	15,21,*,46
		.5	.6974	1.034	-.3878	-.5346	1.4422	13	16
		1.0	.9692	.7805	-.3902	-.6092	1.5129	13	17
	-.4643	.11111	.3602	1.6602	-.4282	-.30625	1.1960	22	12
	-.45	0	.1798650	2.35976	-.53095	0	.84888	21	
	-.40	0	.1955875	2.26737	-.45347	0	.88694		
	-.35	0	.2116425	2.18177	-.38181	0	.92351		
	-.30	0	.2280125	2.10220	-.31533	0	.95866		
	-.25	0	.2446800	2.02802	-.25350	0	.99243		
	-.20	0	.2616350	1.95866	-.195866	0	1.0249		
	-.15	0	.2788625	1.89364	-.14202	0	1.0561		
	-.1107	1.0	1.171	.6763	-.07487	-.4574	1.5819	23	63
	-.10	0	.2963500	1.83255	-.091627	0	1.0862	21	
	-.05	0	.314085	1.77503	-.044375	0	1.1150	21	
Solid	0	-0.0904	0	3.4977	0	1.1059	0	13,19,24	11,237,29
		-.0868	.0581	2.9702		.7658	.3451		
		-.0826	.0870	2.7628		.6305	.4807		
		-.0741	.1296	2.5097		.4667	.6505		12,237,29
		-.0654	.1637	2.3358		.3568	.7647		
		-.0476	.2202	2.0919		.2083	.9213		
		0	.3321	1.7207		0	1.1429	19,20,21,23	12,237,13,*,46
		.05263	.4259	1.4891		-.1167	1.2684	19,24	237,29
		.11111	.5120	1.3199		-.1936	1.3516	19,22,24	237,12,29
		.1765	.5942	1.1876		-.2489	1.4113	19,24	237,29
		.25	.6753	1.0785		-.2908	1.4566		
		.33333	.7575	.9851		-.3234	1.4924		
		.4286	.8418	.9037		-.3500	1.5215		

*Pages in tables of ref. 21 are not numbered.

TABLE V. - Concluded. SUMMARY OF DIMENSIONLESS PARAMETERS FOR THE DIFFERENT GEOMETRIES

(d) Concluded. Porous wedge

	$f_{b,w}$	Eu	$f_b''(0)$	$\frac{\delta^*\sqrt{Re_x}}{x} = B$	Φ_b	$\pi_{b,x}$	T_b	Additional information	
								Reference	Page
Solid	0	0.05	0.8998	0.854	0	-0.3647	1.5370	20,23	13,14
		.8667	1.0225	.7654		-.3906	1.5652	19,24	237,29
		1.0	1.2328	.6479		-.4198	1.5972	13,19,20,21,23	14,237,15,*,46
		1.5	1.4937	.5427		-.4418	1.6213	19,24	237,29
		4	2.4049	.3440		-.4733	1.6546		
		∞	∞	0					
Suction	0.05	0	0.3502575	1.88951	0.041737	0	1.1695	21	
	.1		.3686725	1.82098	.081049		1.1952		
	.15		.3872975	1.57498	.11812		1.2200		
	.2		.4061200	1.53129	.15313		1.2438		
	.25		.4251350	1.48977	.18622		1.2667		
	.3		.444335	1.45025	.21754		1.2888		
	.35		.4637100	1.41257	.24720		1.3100		
	.4		.4832525	1.37664	.27533		1.3305		
	.45		.502960	1.34231	.30202		1.3503		
	.5		.5228225	1.30949	.32737		1.3693	21,23	*,46
	.5	1.0	1.5418	.5419	.2710	-.2837	1.6710	23	63
	.5005	.11111	.7030	1.0612	.2951	-.12513	1.4920	22	12
	.6	0	.562995	1.24801	.37440	0	1.4052	21	
	.7		.603725	1.19151	.41703		1.4387		
	.8		.644970	1.13945	.45578		1.4698		
	.9		.686695	1.09130	.49108		1.4988		
	1.0		.7288675	1.04667	.52334		1.5258	21,23	*,46
	1.095	1.0	1.9550	.4440	.4862	-.1971	1.7360	23	63
	1.1	0	.771455	1.00521	.55286	0	1.5508	21	
	1.2		.814430	.96658	.57995		1.5744		
	1.3		.8577600	.93056	.60486		1.5964		
	1.4		.9014350	.89682	.62777		1.6168		
	1.5		.9454225	.86523	.64892		1.6360	21,23	*,46
	1.8828	.11111	1.2271	.6967	.6513	-.05393	1.7098	22	12
	1.9265	1.0	2.6080	.3485	.6714	-.1215	1.8178	23	63
	2.0	0	1.169425	.73335	.73335	0	1.7152	21	
	2.5	0	1.398825	.63380	.79225	0	1.7732	21	
	2.684	1.0	3.2400	.2900	.7726	-.0841	1.8792	23	63
	3.0	0	1.632225	.55640	.83460	0	1.8183	21,23	*,46
	3.5	.11111	2.1332	.4363	.8484	-.02115	1.8614	22	12
	4.0	0	2.107400	.44470	.88940	0	1.8743	21	
	5.0		2.58990	.38869	.92172		1.9097	21,23	*,46
	6.0		3.077075	.31403	.94209		1.9326	21	
	6.4139	.11111	3.8794	.2640	.9407	-.00774	1.9427	22	12
	10.0	0	5.048525	.19530	.97650	0	1.9720	21	

*Pages in tables of ref. 21 are not numbered.

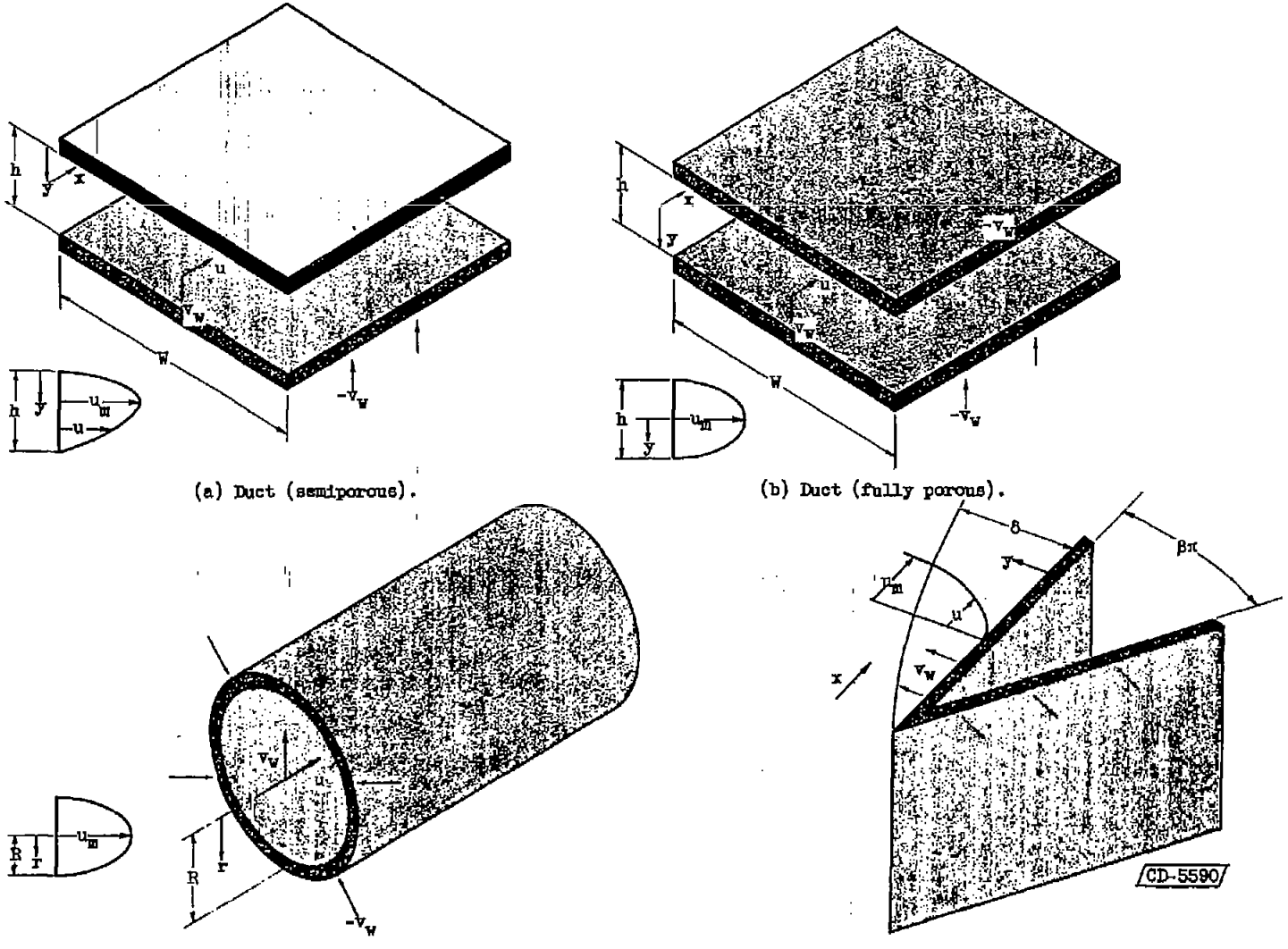

(a) Duct (semiporous).

(b) Duct (fully porous).

(c) Porous tube.

(d) Boundary layer on porous wedge.

Figure 1. - Geometries of various flow configurations.

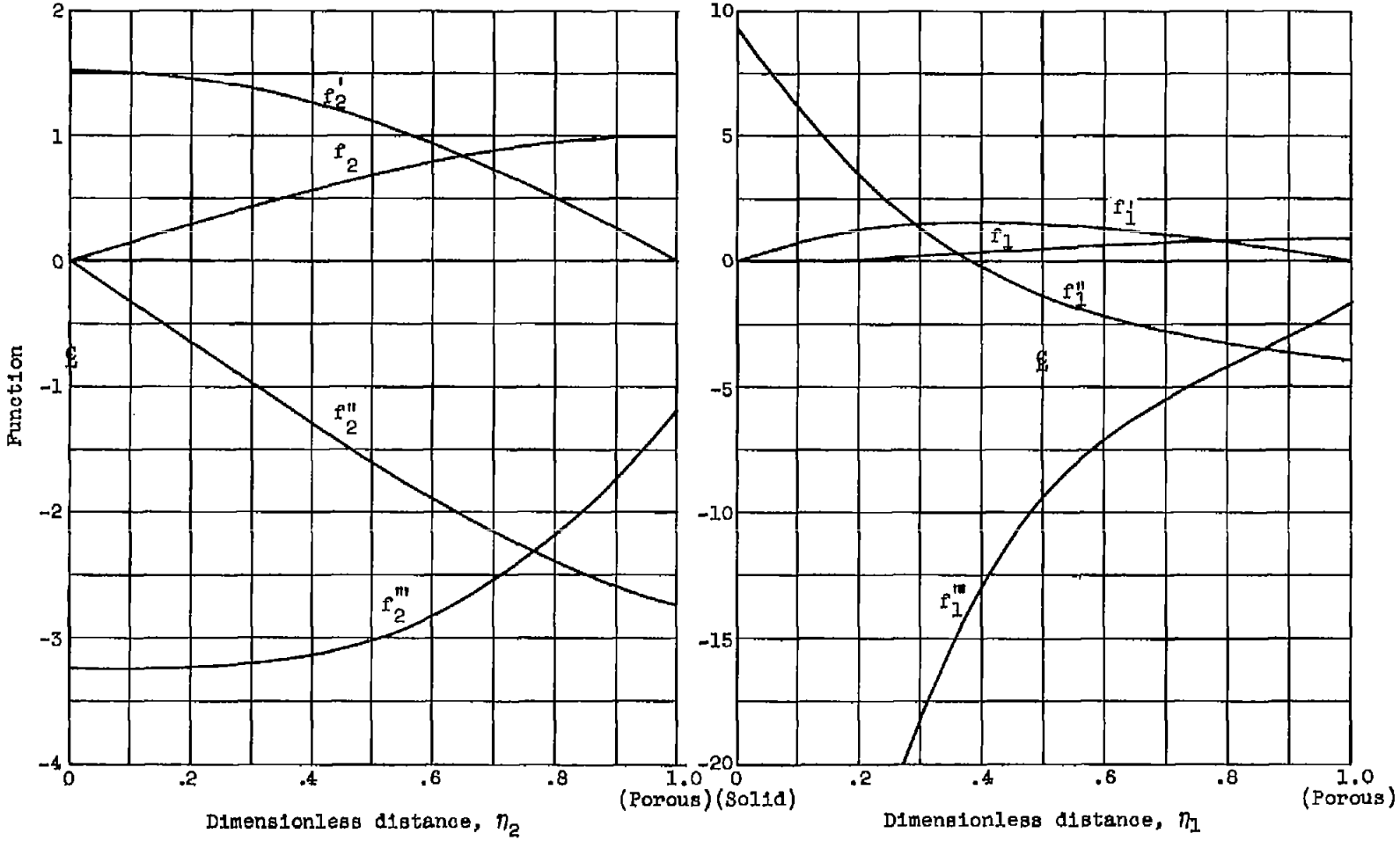

(a) Fully porous duct; wall Reynolds number $Re_{2,w}$, -10.

(b) Semiporous duct; wall Reynolds number $Re_{1,w}$, -8.

Figure 2. - Representative solution of appropriate equation (7).

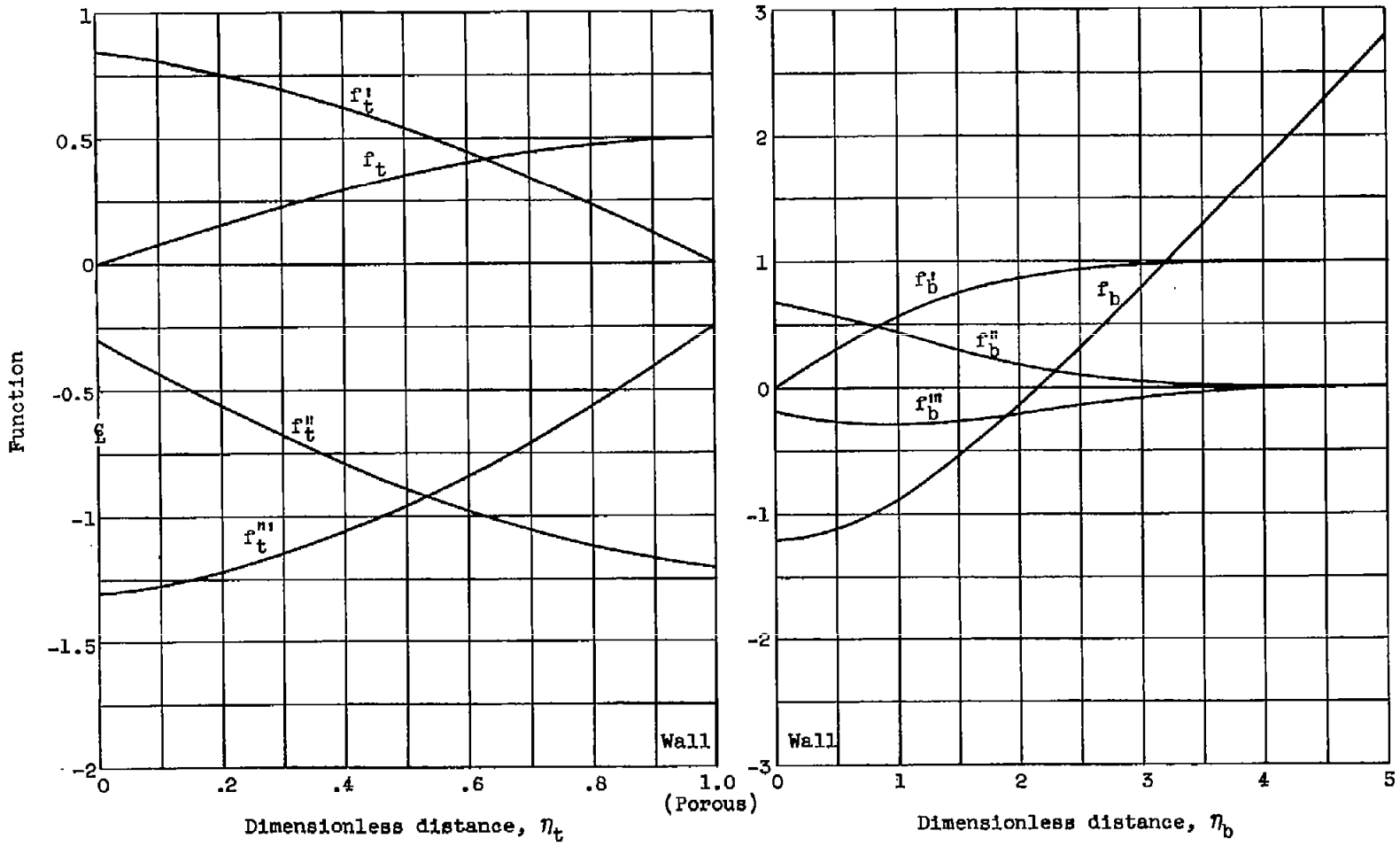

(c) Porous tube; wall Reynolds number $Re_{t,w}$, -10.

(d) Boundary layer; Euler number, 1.0; wall boundary-layer function $f_{b,w}$, -1.198.

Figure 2. - Concluded. Representative solution of appropriate equation (7).

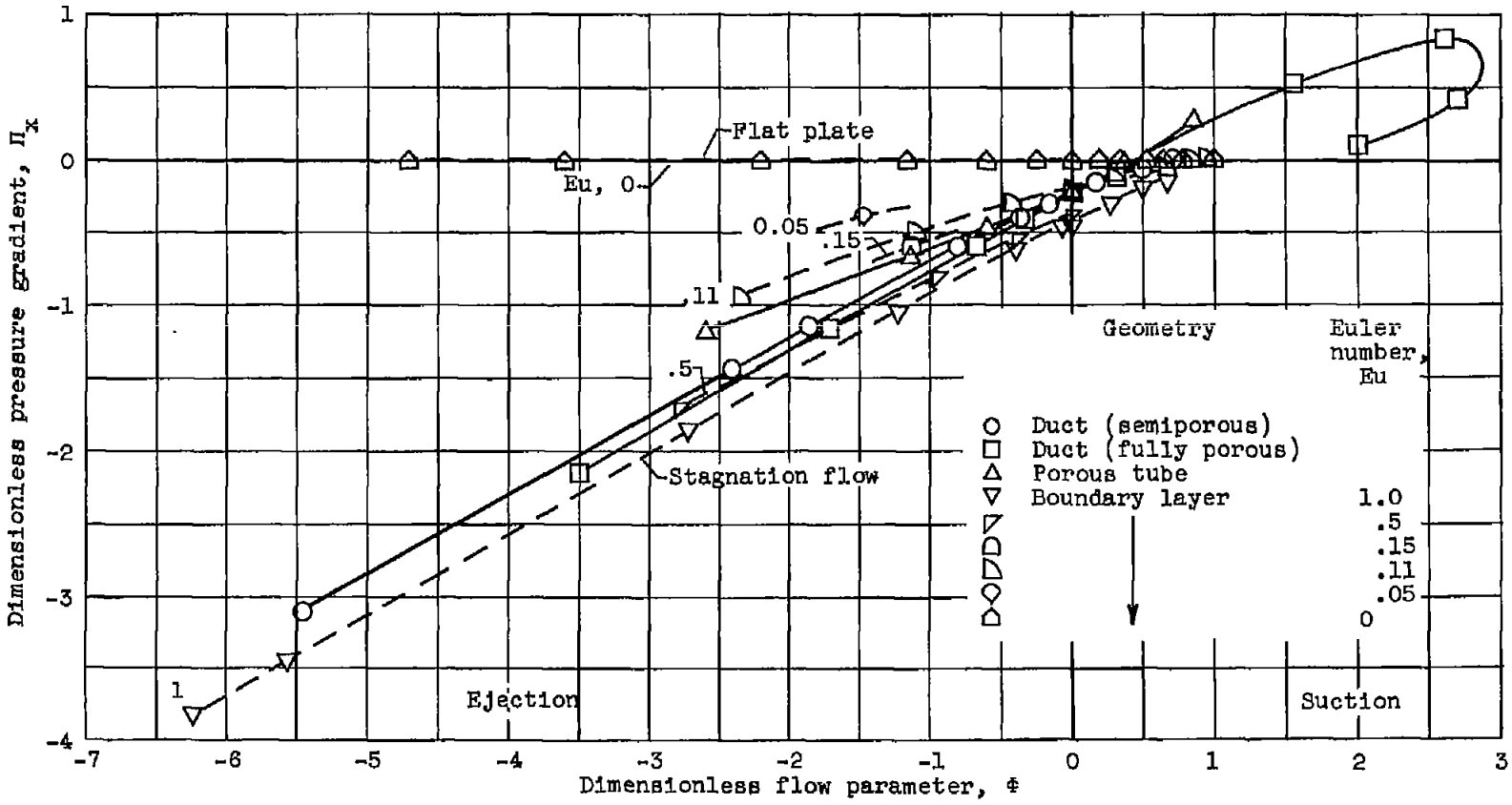

(a) Abscissa scale, $-7.0 \leq \Phi \leq 1.0$.

Figure 3. - Dimensionless pressure gradients and flow parameters for various geometries.

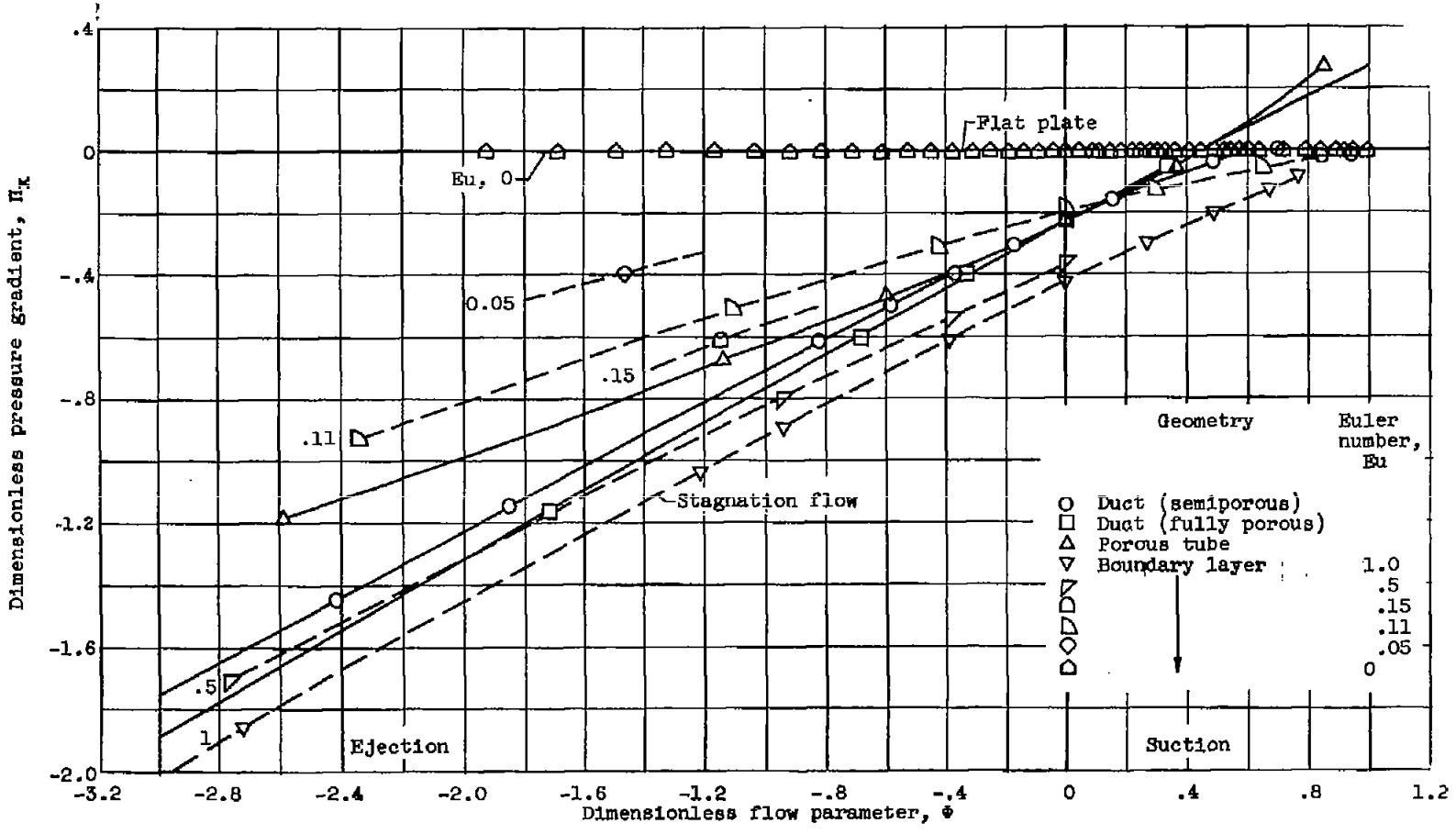

(b) Abscissa scale, $-3.2 \leq \Phi \leq 1.2$.

Figure 3. - Concluded. Dimensionless pressure gradients and flow parameters for various geometries.

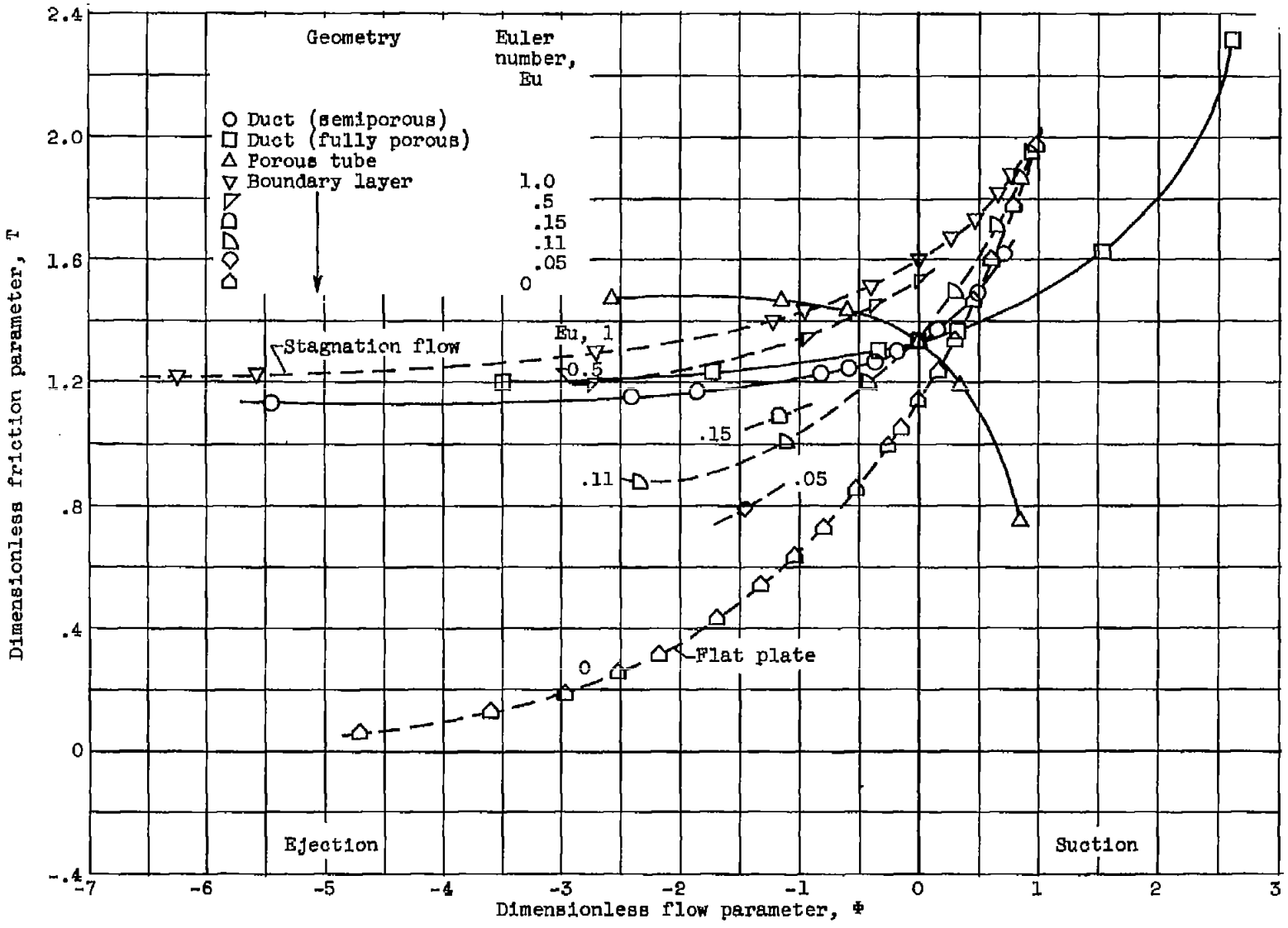

Figure 4. - Wall friction for various geometries.

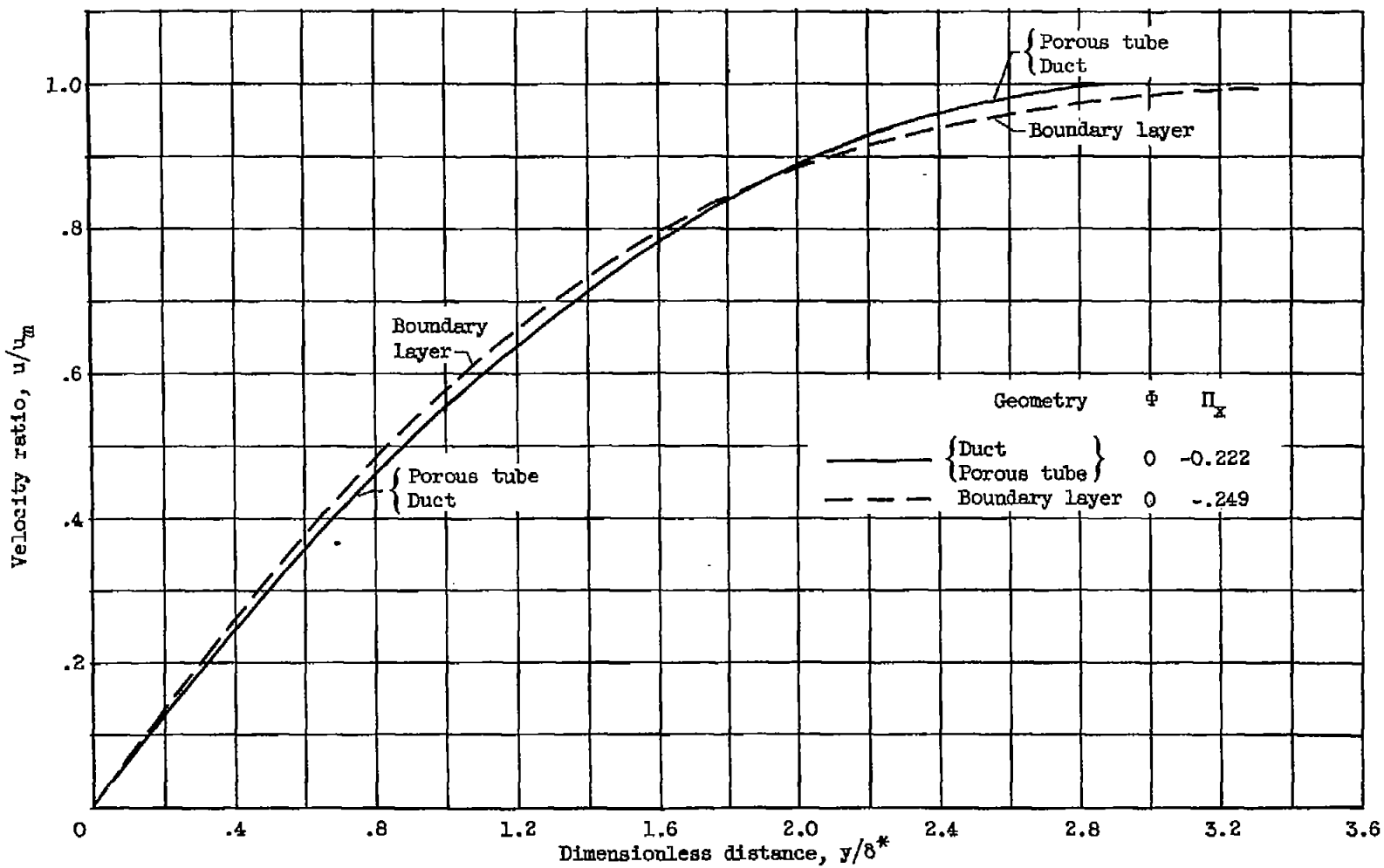

(a) Flow parameter Φ, 0; pressure-drop parameter Π_x, $\approx$-0.2.

Figure 5. - Velocity distribution for various geometries.

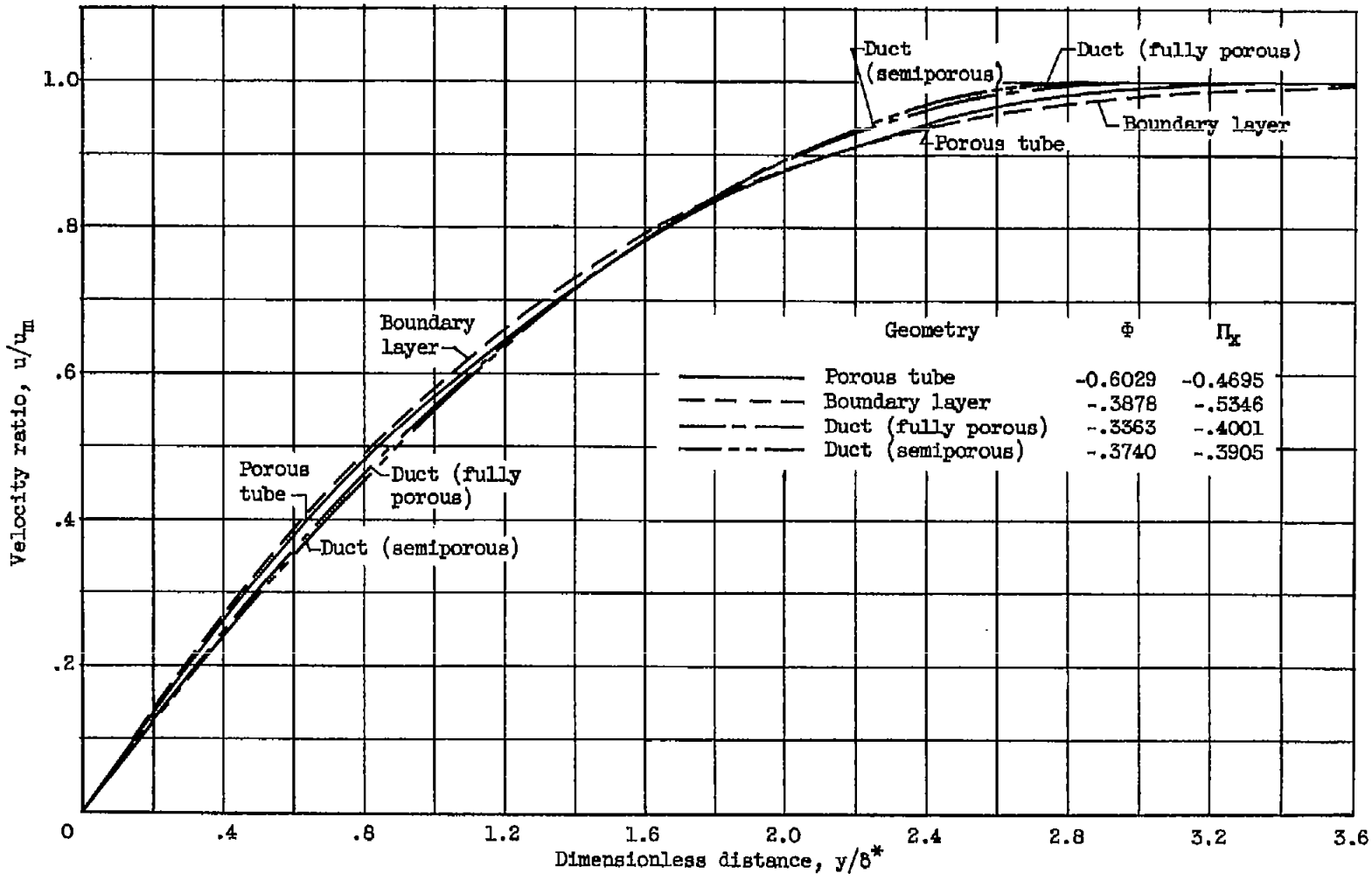

(b) Flow parameter Φ, ≈-0.4; pressure-drop parameter Π_x, ≈-0.45.

Figure 5. - Continued. Velocity distribution for various geometries.

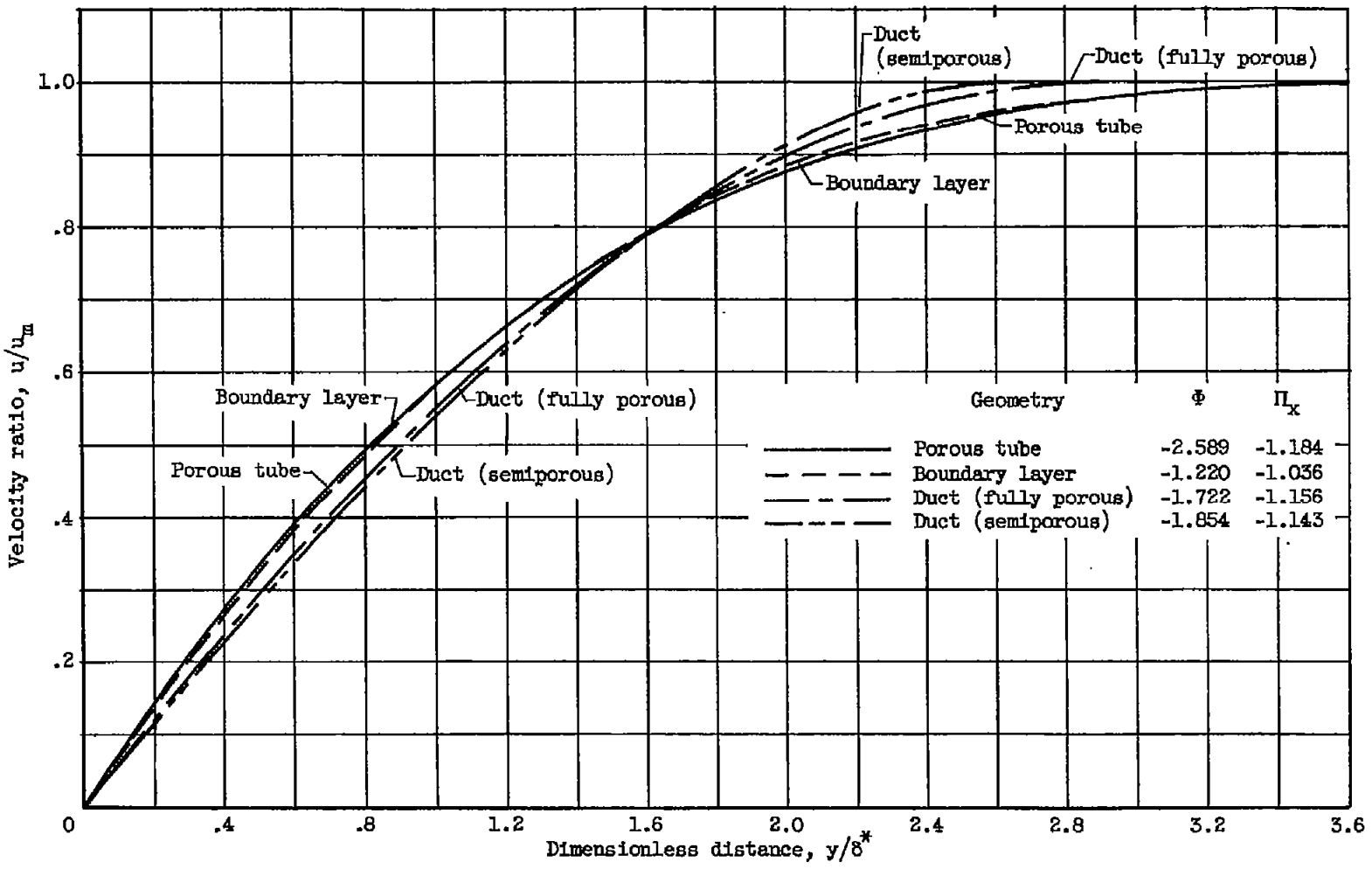

(c) Flow parameter Φ, ≈ -2; pressure-drop parameter Π_x, ≈ -1.1.

Figure 5. - Continued. Velocity distribution for various geometries.

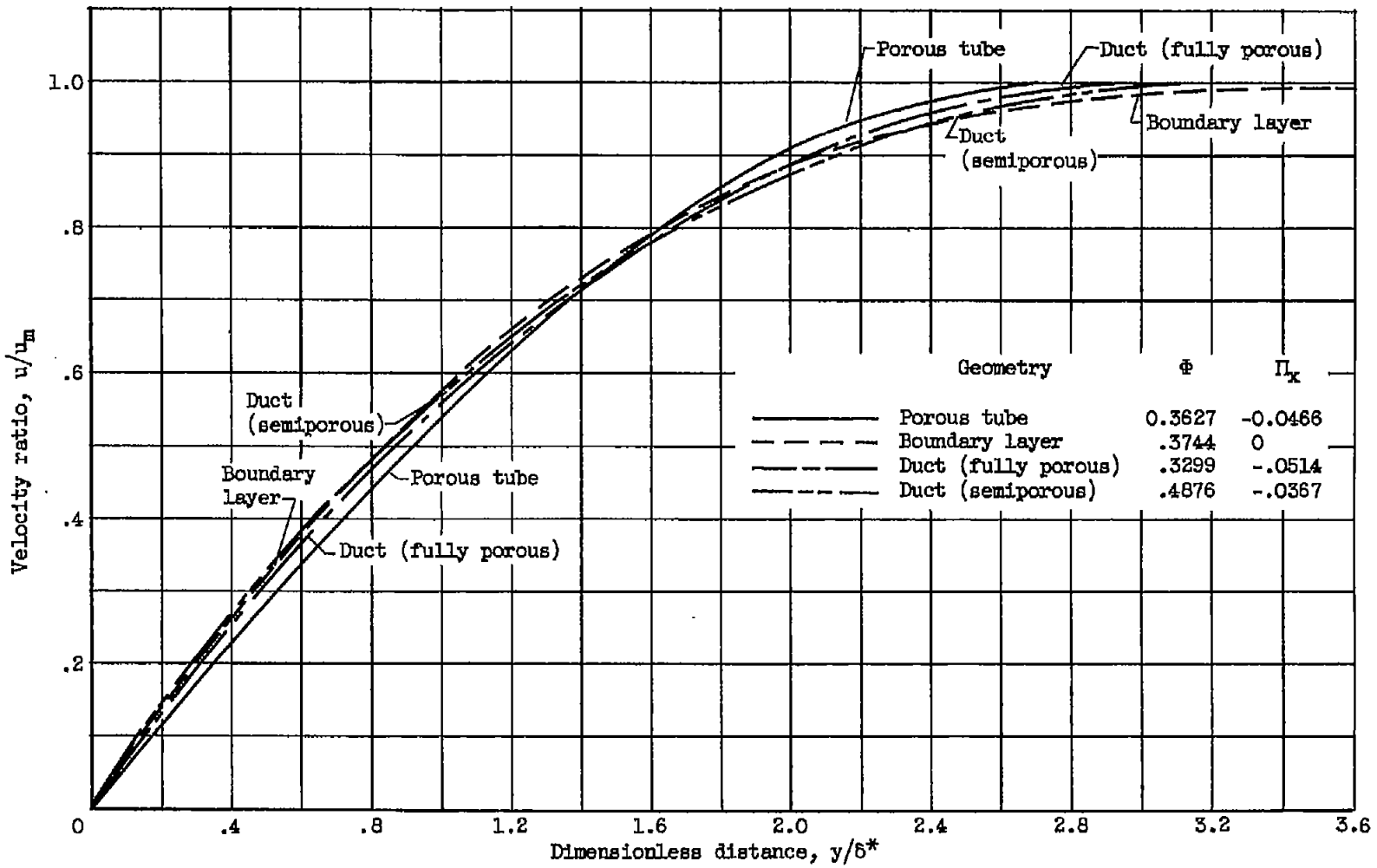

(d) Flow parameter Φ, ≈ 0.5; pressure drop parameter Π_x, ≈ -0.04.

Figure 5. - Concluded. Velocity distribution for various geometries.

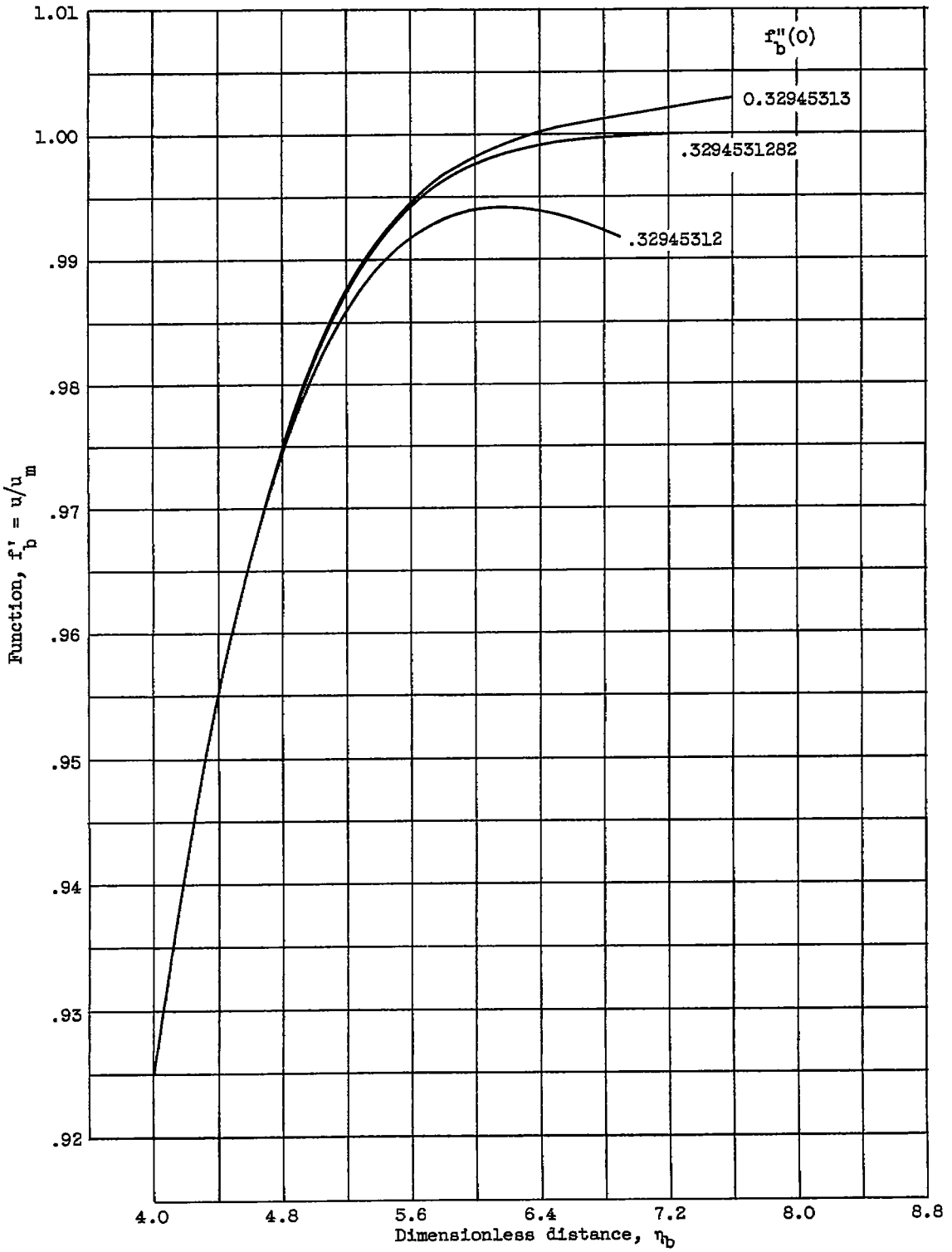

Figure 6. - Velocity profile f'_b for boundary layer for different input values. Euler number Eu, 1; flow rate parameter $f_{b,w}$, -3.

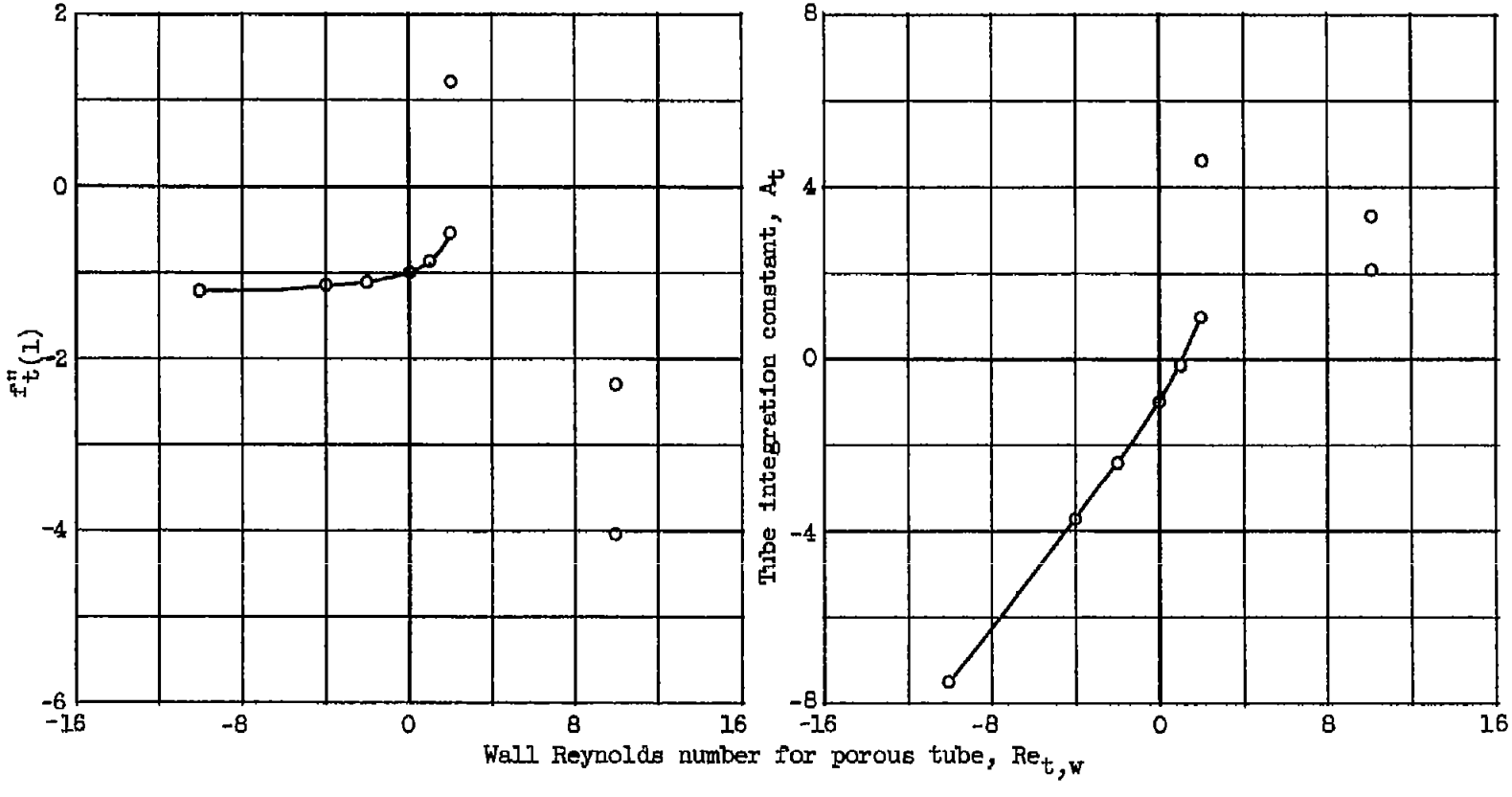

Figure 7. - Numerical results for porous tube.

NACA - Langley Field, Va.